# "COMPARATIVE STUDY OF MECHANICAL AND MICROSTRUCTURE PROPERTIES OF AA6082-T6 USING CMT AND FSP OVER CMT WELDING"

A PROJECT REPORT

SUBMITTED IN THE PARTIAL FULFILMENT OF THE
REQUIREMENTS FOR THE AWARD OF DEGREE
OF

MASTER OF TECHNOLOGY
IN
PRODUCTION ENGINEERING

SUBMITTED BY:

**MEHUL PATHAK**
**(2K21/PRD/07)**

Under the supervision of

**Prof. Reeta Wattal**             **Dr. RAVI BUTOLA**
Professor                          Assistant Professor
Department of Mechanical Engineering   University School of Automation
Delhi Technological University     & Robotics (USAR), GGSIP University

**DEPARTMENT OF MECHANICAL ENGINEERING**
DELHI TECHNOLOGICAL UNIVERSITY
(Formerly Delhi College of Engineering)
Bawana Road, Delhi – 110042

**JUNE, 2023**

<u>**CANDIDATE'S DECLARATION**</u>

I, Mehul Pathak , Roll No. 2K21/PRD/07 of M.Tech (Production Engineering), hereby certify that the project Dissertation titled "**Comparative study of Mechanical and Microstructure properties of AA6082-T6 using CMT and FSP over CMT welding**" which is submitted by me to the Department of Mechanical Engineering, Delhi Technological University, Delhi in partial fulfilment of the requirement for the award of the degree of the Master of Technology, is original and not copied from any source without proper citation. This work has not previously formed the basis for the award of any Degree, Diploma Associateship, Fellowship or other similar title or recognition.

Place: Delhi                                  Mehul Pathak

Date:                                       2K21/PRD/07

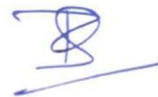                                                      M.Tech (Production Engineering)

                                                      Delhi Technological University

## <u>CERTIFICATE</u>

I hereby certify that the Project Dissertation titled "**Comparative study of Mechanical and Microstructure properties of AA6082-T6 using CMT and FSP over CMT welding**" which is submitted by MEHUL PATHAK, 2K21/PRD/07, Mechanical Engineering Department, Delhi Technological University, Delhi in partial fulfilment of the requirement for the award of the degree of Master of Technology, is a record project work carried out by the student under my supervision. To the best of my knowledge this work has not been submitted in part or full for any Degree or Diploma to this University or elsewhere.

Prof. Reeta Wattal                                    Dr. Ravi Butola

**SUPERVISOR**                                      **SUPERVISOR**

Professor                                                    Assistant Professor

Department of Mechanical Engineering        University School of Automation

Delhi Technological University                    & Robotics (USAR), GGSIP University

Place:

Date:

# ACKNOWLEDGEMENT

First of all, I wish to convey my deep gratitude and sincere thanks to my M.Tech supervisor, Prof. Reeta Wattal and Dr. Ravi Butola for giving me an opportunity to pursue this research work at Delhi Technological University. I feel very fortunate that I got an opportunity to work under his supervision. I would like that thank all the staff and faculty members of Mechanical Engineering Department for their continuous help, encouragement and support.

Finally, I dedicate my work to my parents. My sincere thanks to my mother Mrs. Seema Sharma and my father Mr. Dharmendra Kumar Sharma for their unconditional love, support and blessings that greatly helped me carrying out my research work.

MEHUL PATHAK

2K21/PRD/07

M.Tech (Production Engineering)

Delhi Technological University

## **ABSTRACT**

Being light weight, malleable and ductile, good corrosion resistance, good conductor of heat and electricity, aluminium alloys have wide range of application in various types of industries but they are difficult to weld. FSW and CMT are widely accepted techniques for welding of aluminium alloys due to their low heat input and different mechanism. This research focuses on comparative study of CMT welding process and a hybrid welding process which is FSP over CMT. 5 mm thick AA6082 aluminium alloy was selected as base material while looking at compatibility, ER 5356 was selected as a filler wire. Mechanical properties, hardness distribution, and microstructure were studied for both the processes. For FSP, circular profile tool was used with constant 1° tilt angle in clockwise direction. Experiments were conducted on different process parameters with the help of DoE and same were optimized with the help of Taguchi optimization technique. ANOVA was used to find out the percentage contribution of an individual parameter. From optimization, welding current has more effect (67.47% contribution) on the strength of CMT welded specimen compared to other process parameter while tool rotation speed was more effecting (50.45% contribution) on UTS in case of FSP over CMT welded samples. After the tensile test, for CMT sample, the maximum UTS was (192 MPa) 75.88% of the base metal (253 MPa) while for FSP over CMT sample, maximum UTS was (168 MPa) 66.40% of base metal. More UTS was observed (sample no. 7, 8, & 9) at higher current in CMT while UTS was in range of 155-168 MPa for FSP over CMT samples. Hardness test for CMT sample shows that it have the maximum value at HAZ

followed by base metal and weld zone forming M-pattern while for FSP over CMT sample, hardness at TMAZ was highest followed by stir zone and base metal. Moreover, FSP increased the hardness value by 2%. Microstructure analysis for FSP over CMT sample shows that at higher tool rotation speed, tunnel defect was there which was lowering the value of UTS for the same sample. Onion rings can be seen in the stir zone while very fine equiaxed grain structure was there in stir zone. Due to dynamic recrystallization, fine grains were there in the stir region and hence, FSP was successful in increasing the hardness of the CMT welded specimen. Microstructure of CMT samples shows coarser grain structure at HAZ while elongated fine grain structure at weld bead zone. For some samples, lower value of UTS was observed because of gas porosity defects and lack of fusion between the plates. Moreover, FSP successfully removes the gas porosity defects and lack of fusion from the CMT welded sample. Thus conforming the strength not to be lower than its range.

**Keywords:** AA6082, ER5356, CMT, FSP, Taguchi technique, ANOVA, Tensile Test, Microhardness, Microstructure

# TABLE OF CONTENTS

# LIST OF FIGURES

# LIST OF TABLES

# LIST OF ABBREVIATION

ANOVA            Analysis of Variance

AS            Advancing Side

ASTM            American Society for Testing and Materials

BM            Base Metal

CMT            Cold Metal Transfer

CMT-P            Cold Metal Transfer – Pulse mode

CMT-PADV            Cold Metal Transfer – Pulse Advance Mode

CMT-VP            Cold Metal Transfer – Variable Polarity mode

DCEN            Direct Current Electrode Negative

DCEP            Direct Current Electrode Positive

DoE            Design of Experiments

EDM            Electro Discharge Machining

FSP            Friction Stir Processing

FSW            Friction Stir Welding

GFR            Gas Flow Rate

GMAW            Gas Metal Arc Welding

GTAW            Gas Tungsten Arc Welding

| | |
|---|---|
| HAZ | Heat Affected Zone |
| HV | Vickers Hardness |
| MIG | Metal Inert Gas |
| RS | Retreating Side |
| SN Ration | Signal-to-Noise Ration |
| SZ | Stir Zone |
| TIG | Tungsten Inter Gas |
| TMAZ | Thermo-Mechanical Affected Zone |
| TRS | Tool Rotation Speed |
| TTS | Table Traverse Speed |
| UTM | Universal Testing Machine |
| UTS | Ultimate Tensile Strength |
| WAAM | Wire Arc Additive Manufacturing |
| WC | Welding Current |
| WS | Welding Speed |
| WZ | Weld Zone |

# CHAPTER 1

# INTRODUCTION

## 1.1 General Background

Additive manufacturing is one of the key component of Industry 4.0 and under that various techniques are there which make it more promising modern manufacturing technology compare to existing technologies [1]. While welding is an old age techniques, it still plays a vital role in the making of various material joints. In the industrial application like aircraft and marine construction, automobile manufacturing, Railway industry, structural applications etc. welding is almost in every place. Moreover, all these industries are also running towards the use lighter material which can help in weight reduction and can indirectly reduce the fuel consumption thus selecting aluminium for welding purpose [2, 3].

Various types of welding are there according to their application. Welding is a phenomenon in which a joint is established between two metallic plates in as required orientation with the help of heat and pressure and with or without the use of filler material. It is not necessary that in welding, the two metal surfaces have to melt. There are various types of welding and as Additive Manufacturing is an emerging technology, more new types of welding technique has come into picture from which we can either join two material or we can produce a new surface layer by layer. Such type of welding process is Cold Metal Transfer technique of welding which is nothing but an advanced version of Metal Inert Gas (MIG) welding which welds with less spatter and low heat input.

Also, there is another type of solid state welding process in which there is no melting of material while making a joint of similar or dissimilar metals known as Friction Stir Welding (FSW). Similar to principal of FSW, Friction Stir Processing (FSP) is a surface refinement process in which local microstructure changes to get as required properties. The major

difference between FSP & FSW is that the first one is majorly used for surface refinement while the second one is used to join the two metals [4].

## 1.2 Application of aluminium alloy

Aluminium is light in weight but still some of the aluminium alloys exceeds mild steel in terms of strength. Also, it is easy to fabricate as it can be cast, forged, rolled, drawn, hammered, stretched, etc. it has properties like good ductility, corrosion resistance, good thermal and electrical conductivity, high reflectivity, etc. due to all these features, it have a wide variety of applications in sectors such as automobile, building and construction, electronics equipment, shipbuilding and marine construction, aerospace sector, etc. [2, 3].

## 1.3 Types of aluminium

Broadly there are two main category of aluminium alloys, they are Cast aluminium alloys (which have more than 22% alloying elements by composition) and wrought aluminium alloys (which have less than 4% alloying elements by composition). This composition proportion have a significant impact on their mechanical properties like Cast aluminium alloys lacks in ductility while Wrought aluminium alloys have good ductility, corrosion to resistance, conductivity, etc.

Wrought aluminium alloys are designated by a four-digit system (xxxx) where first digit represents the primary alloying element and is frequently used to describe its series, second digit represents the initial alloy variation, while third and fourth number have no meaning but still represents individual alloy variation. Below list describes all grades of wrought aluminium alloy.

a. **1xxx series**: This series represents 99% pure aluminium alloy and have relatively low strength. They have good ductility, formability, corrosion resistance, high thermal and electrical conductivity and can be welded by any method. They are used in chemical and food packaging and processing industries.

b. **2xxx series**: In this series, primary alloying element is copper and thus, they have good strength because copper provides solution strengthening and precipitation hardening. They are generally used where good strength-to-weight ratio is required.

They have poor resistance to atmospheric corrosion but have good fatigue resistance. Used in aerospace structural parts, heavy duty forging, automotive parts.

c. **3xxx series**: In this series, primary alloying element is Manganese. This series have medium strength but have high ductility and formability. They are also good for welding and deep drawing and have very high corrosion resistance. Used for cladding, chemical tanks, food handling containers.

d. **4xxx series**: In this series, primary alloying element is Silicon. They have less resistance to atmospheric corrosion but due to addition of silicon, they have excellent flow characteristics and hence, they are used in piston forging and valve bodies. They are also used to join different series of aluminium as welding wire.

e. **5xxx series**: In this series, primary alloying element is Magnesium. They have high impact strength, toughness, excellent atmospheric and seawater resistance and hence widely used in marine applications. Used for cladding, structural members, architectural purposes.

f. **6xxx series**: In this series, Magnesium and Silicon are the main alloying elements. They have excellent precipitation-hardening ability. They have high strength with excellent corrosion resistance. They are easy to extrude and are widely used to produces complex shapes. They have marine, architectural, and general purpose application.

g. **7xxx series**: In this series, Zinc is the main alloying element. It is the strongest wrought aluminium alloy series. Addition of zinc decreases workability and machinability, higher strength compensates it. They have relatively poorer atmospheric resistance and are less tough. They are widely used in aircraft forging, military mobile equipment, and in highly stressed parts.

h. **8xxx series**: This series is made up of variety of alloys and are used for specific applications like high-temperature usage, reduced densities, and other special features. They are used in helicopters parts and space applications [5].

**1.4 Welding of aluminium:**

There are basically two main category in which welding of aluminium done. They are solid-state welding process in which fusion occur below the melting point of base metal and liquid-state welding process in which fusion occur above the melting point of base metal. In liquid-

state welding process, majorly Gas Metal Arc welding (GMAW) & Gas Tungsten Arc welding (GTAW) are used, since they have wide range of application and acceptance in industry. Since aluminium alloys have high conductivity, high coefficient of thermal expansion, surface oxide generation, aluminium alloys are more difficult to weld than other materials. During welding of aluminium alloys, ambient gases trapped in the weld and thus porosity occurs, which decreases the weld strength [6]. Also, welding of dissimilar material i.e., aluminium to other material is also a challenging task since there is huge difference between their thermos-physical property and at elevated temperatures, formation of Al-Fe layer also occurs [7]. For countering these problems, CMT welding process is widely used to weld aluminium-to-aluminium or aluminium-to-steel [7 - 10, 18]. CMT have low heat input and does spatter free welding and can weld thin sheets also. It has heat input lower than GMAW process [11]. While Friction Stir Welding (FSW) comes under solid-state welding, is also used to join the aluminium alloys [12 - 14]. Similar to the principle of FSW, Friction Stir Processing (FSP) is a surface refinement process in which we can get desired properties by modifying the microstructure up to some depth. FSP is also used as a post-processing technique to upgrade the properties of weldment by its stirring effect [15].

**1.5 Cold Metal Transfer (CMT)**

Cold Metal Transfer welding (invented by Fronius company) is an advance type of conventional MIG welding process in which heat input is less compared to the same while wire is retracted in short circuiting phase in place of continuous movement. This welding process has been successfully used for welding of similar and dissimilar metals [16]. In this process, as the electrode tip makes forward movement and touches the molten pool, the servomotor used to control the welding torch reverse the direction of the wire and it moves backward by digital process control. During the droplet transfer, the current value touches the near-zero mark and thus, generation of spatter is avoided. The re-ignition of the arc occur immediately as the droplet transfer completes and the electrode wire is provided with a forward motion again and the whole cycle repeats [17]. Talking about the backward motion of the feed wire during the short circuiting stage, it results in spatter free process with better weld bead, good penetration, and low heat-input. Thus, CMT welding has a wide range of applications in the field of additive manufacturing, cladding, crack repair welding, and composite joint pin fabrication [18]. The basic diagram of CMT has been shown in Fig. 1.1

in which two aluminium alloy AA6082 plates have been jointed in a butt configuration using CMT torch.
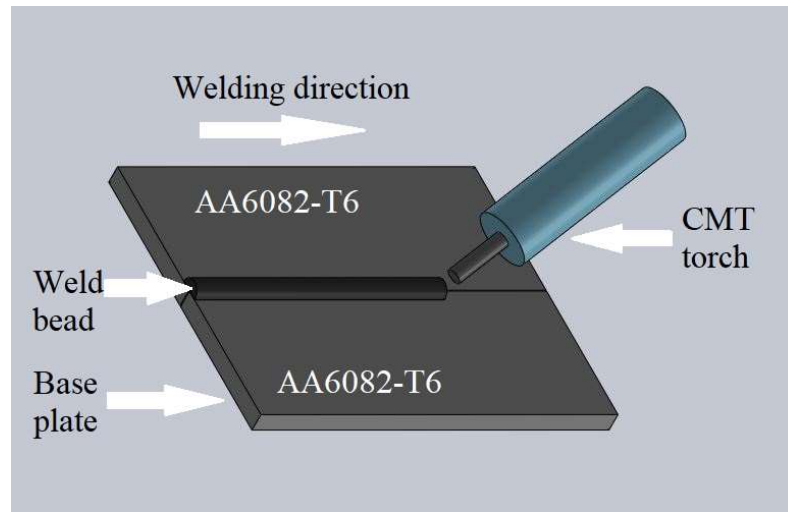


Figure 1.1. Cold Metal Transfer process

The CMT welding process works in a cycle and it can be defined as that time interval in which the liquid droplet of electrode deposited in the weld pool. To investigate the energy distribution of CMT droplet transfer process during all the phases, inspection of current and voltage waveform are required. Generally, the CMT cycle is divided into three phases and they are as follows:

1. Peak current phase: During this phase, the electrode wire heats up easily and forms the droplet since in this phase, there is constant arc voltage along with high current pulses which helps in arc ignition.

2. Background current phase: During this phase, the current is intentionally reduced so that globular droplet transfer can be prevented formed on the wire tip up to the short circuiting phase.

3. Short-circuiting phase: During this phase, the arc voltage is reduced to zero and on the other hand, a retraction signal is send to the wire feeder system which help in wire backward motion. Also, liquid fracture occurs in this phase and material droplet transfers to the weld pool [19].

The droplet detachment process of CMT is completely different from conventional process. In conventional process, the feed wire is continuously moved forward until a short circuit

occurs and welding current increases which continue the arc ignition while in CMT, the wire is first pushed forward and then retracted, thus backward and forward motion of wire resembles oscillating feed wire system with a frequency up to 70 Hz [20]. During arcing period in CMT (Fig. 1.2), first there is a forward movement of filler wire (Fig. 1.2(a)), secondly, the welding current decreases and arc extinguish, since the wire tip dips in weld pool (Fig. 1.2(b)), thirdly, retraction movement of wire occurs instantaneously with the help of servomotor during the short circuit and thus droplet detachment occurs (Fig. 1.2(c)), and finally the wire drives back and whole process repeats itself (Fig. 1.2(d)) [11].
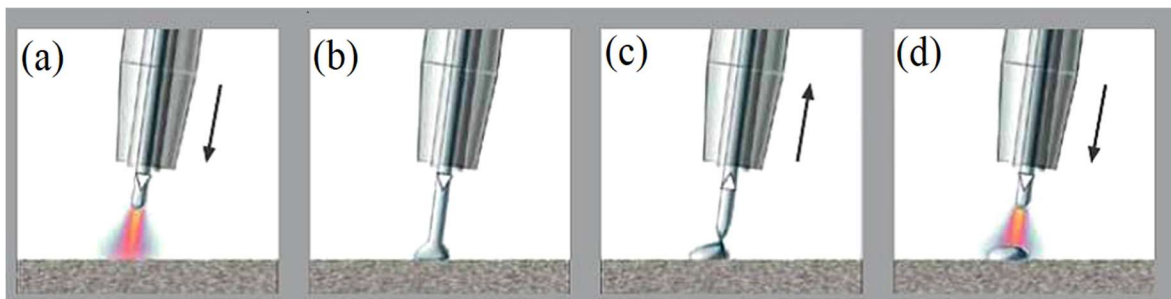


Figure 1.2. Phases of CMT process (a–d) [11].

In CMT, the energy distribution during short-circuit stage in a welding cycle is about 5% while in MIG welding it is around 40%, thus making it more suitable for aluminium alloys with lower heat input, less spatter, and high deposition rate. CMT machine also have different arc modes which are used for different applications. Variable polarity CMT (CMT-VP) mode, CMT pulse (CMT-P) mode are some of the few. Under CMT-VP arc mode, the machine switches between DCEP phase and DCRN phase and hence, influences the arch stability and wire melting rate. This mode have higher deposition rate with no increase in heat input, better thermal management and minimal distortion. CMT-P mode combines of pulse and conventional CMT welding process. High pulse current level are generated during the welding stage which induces more heat input for molten pool and can be easily adjusted and controlled during CMT-P mode compared to conventional CMT welding process [21].

## 1.6 Friction Stir Processing (FSP)

Friction Stir Welding is a solid-state process in which joint between two metals occur below their melting temperature. This process is carried out by using a non-consumable tool with a well-defined profile, pushed into the adjacent edges of the base metal and translated along

the joint line [22]. There are majorly two important function of the FSW tool. First is the heating the base plate with the help of friction and second is the material movement which take place with the help of plastic deformation and material flow. Identical to principal of FSW, FSP is a local microstructure modification technique through which we can get desired properties by modifying the microstructure of specimen to a certain depth. During this process, a specifically designed, continuously rotating non-consumable tool shoulder with extruded pin or pin-less profile is plunged in butt joint and travels along joint line direction with constant rate in to the base metal which is clamped in proper position. The pin is slightly shorter than the required weld depth. The downward thrust and rotation of shoulder and pin of the tool heats up the metal surrounding which leads to recrystallization and causes the softening and flow of metal without melting. Extreme plastic deformation occurs due to heat produced by friction results in significant changes in microstructure in the processed zone. The zone which are evolved during FSP consist of stir zone (SZ), thermo-mechanical affected zone (TMAZ), and heat affected zone (HAZ) as shown in Fig. 1.3. Maximum plastic deformation area of FSP is the SZ and thus, it results in fine grain size structure. The tool rotates from advancing side (where translator vector and angular velocity vector are in same direction) to the retreating side (where they are in opposite direction) while material flows from retreating side to advancing side. The joints between the two pieces establish without melting and degree of mixing decides the strength of the joint [4, 13, 14]. FSP done over CMT in this research have been shown in Fig. 1.4. In this figure, a non-consumable tool has been shown which is rotating and travelling along joint line. Before FSP, a CMT weld has been done in butt configuration. FSP has been successfully used to eliminate defects in the fusion welds. Due to defect removal, there is increment in the tensile strength, microhardness, corrosion resistance, etc. [23, 24].
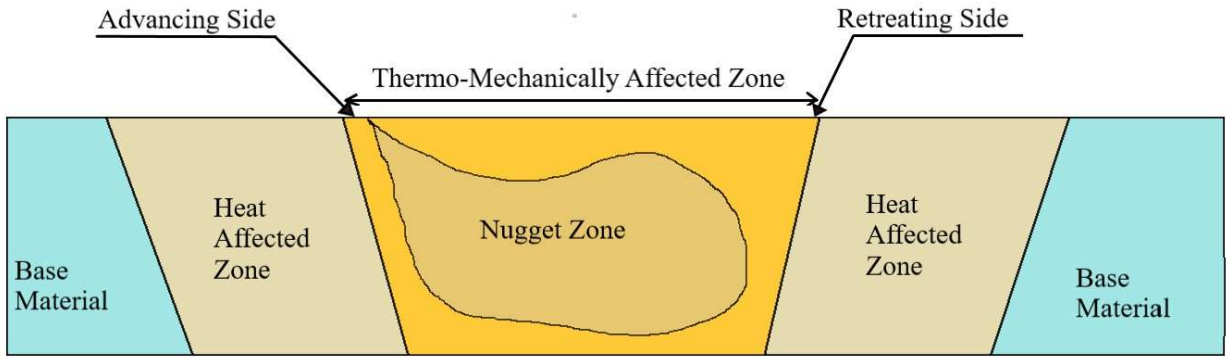
Figure 1.3. Different zone in FSP
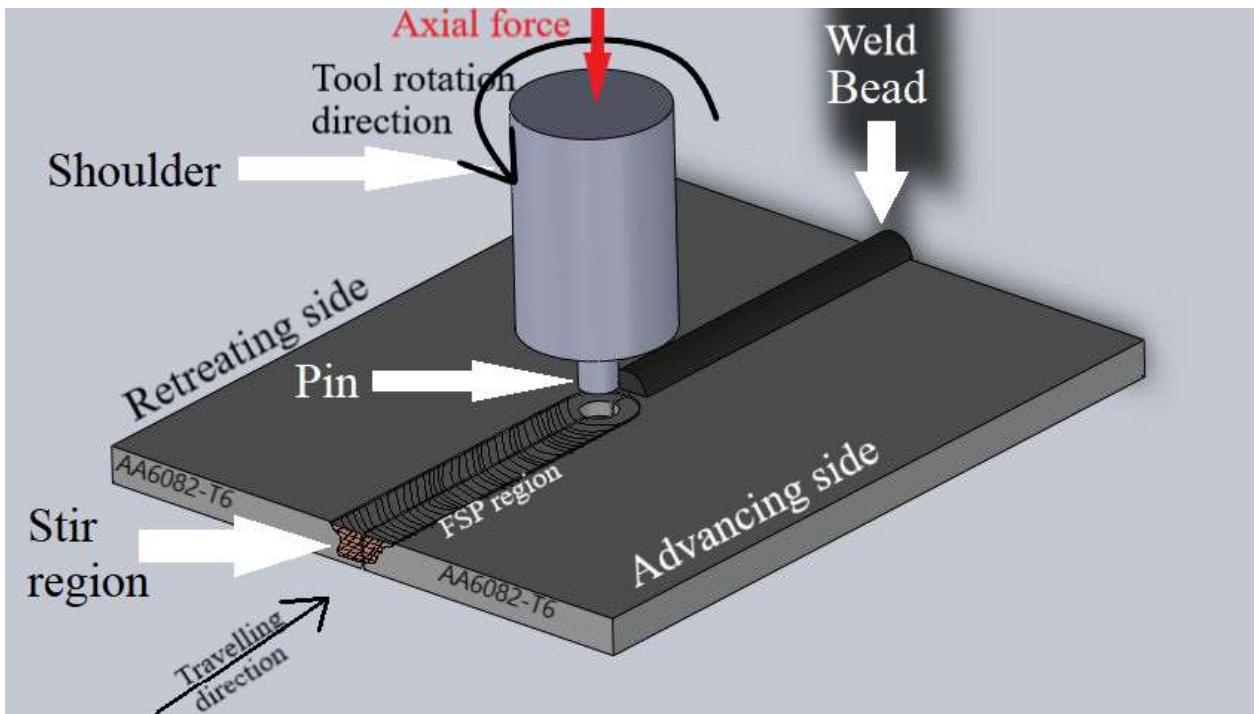


Figure 1.4. FSP over CMT

# CHAPTER 2

# LITERATURE REVIEW

In this research, AA6082 aluminium alloy has been butt welded using ER5356 filler wire by using two techniques. First one is CMT welding process and second is FSP over CMT process. Aluminium alloys are more attractive compared to other material alloy in industrial work, construction work [25], manufacturing and fabrication due to its various properties. But as they have various properties, they are also hard to weld alloys. CMT and FSP are two different techniques by which welding and refinement of aluminium alloys have been done respectively. Both are low heat input techniques. CMT is an advanced version of MIG welding process and welds spatter free while FSP works on the principal of FSW welding process and it refines microstructure upto certain depth to get desired properties. Various studies have been done in past over them as written below in tabular form in Table 2.1.

Table 2.1 Literature review in Tabular form

| Author - Year | Material | Welding technique | Process Parameters | Conclusion |
|---|---|---|---|---|
| R. Cao et al. (2013) [7] | Aluminum alloys (AA6061, AA7075 and AA5183) and mild steel (Q235) | CMT | Wire-feed speed, Welding speed, Deviation distance, Voltage, Coating, Wire, Aluminum base metal | Wire type is one of the most influential process parameter Joint strength depends upon thickness of intermetallic layer and HAZ and can be controlled by controlling the heat input (increases with increase in heat input, after 200 J/mm it decreases). |
| S. Babu et al. (2018) [8] | aluminum alloy (AA 2219) and | Friction Stir Welding and CMT | Coating Thickness, | Sound weld build between aluminum and stainless steel |

| | | | | |
|---|---|---|---|---|
| | stainless steel (AISI 321) | | Average grain size, Surface roughness, Contact angle | Thickness of intermetallic layer decreases as the aluminum coating thickness increases Optimum thickness for highest tensile strength was 0.6 mm |
| S.S. Sravanthi et al. (2019) [9] | 5052 Aluminum alloy, mild steel | MIG, CMT | Weld speed, wire feed rate | Al-Fe-Si IMC layer formed by both the process, the layer was thick and Aluminum rich in MIG sample while it was thin and Iron rich in CMT sample. |
| Shanglu Yang et al. (2013) [10] | 6061-T6 aluminum alloy, zinc coated low carbon steel, ER4043 filler wire | CMT | Lap Presetting Gap and Offset distance | Weld strength increases as the lap presetting gap size increases and decreases by increases in off distance. As the gap was increased to some extent, zinc coating accumulates there which was stopping the intermetallic layer formation. |
| S. Sivabalan et al. (2022) [12] | Al 6082 aluminum alloy | FSW | Tool rotation speed, tool traverse speed | Weld region has fine grains while base metal has coarser grains structure. Nugget zone has higher hardness value compared to HAZ and parent material. |
| P. K. Thimmaraju et al. (2016) [13] | Al 6082 aluminum alloy | FSW | Different Tool profile (triangle, square, hexagonal) | As the number of sides of the tool profile increases, there is reduction in grain size in weld zone and thus, increase in tensile strength can be seen. |
| Liang Zhang et al. (2022) [21] | 5A56 Aluminum alloy | CMT, CMT-P, CMT-VP | Arc mode, arc voltage, wire feed speed | CMT-VP has better thermal management ability, lower heat input, construct fine equi-axed grains and smoother profile with having better mechanical properties compared to CMT and CMT-P mode. |

| E M Stanciu et al. (2017) [26] | S235JR low carbon steel | CMT, Metal Arc Gas | Welding speed, Weld bead width | Weld bead profile and heat affected zone got directly affected by welding speed High welding speed can cause reinforcement which gives poor penetration |
|---|---|---|---|---|
| Xizhang Chen et al. (2018) [27] | 6061-T6 aluminum alloy | CMT | Wire feeding speed, Current, Voltage, Arc mode | Cross sectional width and height can get affected by process parameters as well as shape feature (shape curvature) Increase in wire feeding speed as well as shape curvature can adversely affect the stability of the weld. |
| Rajesh Kannan A et al. (2019) [28] | AISI 316L stainless steel | CMT | Arc length correction | As arc length correction increased, the top reinforcement and strength of weld, both increases. 10% arc length correction was optimum for getting best weld. |
| A. Rajesh Kannan et al. (2022) [29] | AA5052-H32 & AA6061-T6 aluminum alloy | CMT | Welding current, arc voltage, welding speed, wire feed speed, arc length correction, heat input | Successfully welded the two material with average hardness variation of $88 \pm 6$ HV in weld zone Better joint efficiency compared to other welding techniques joining dissimilar material |
| A. Gomez Ortega et al. (2017) [30] | 1050 Aluminum plate, ER4043 filler wire | WAAM using Cold Metal Transfer | Average power, travel speed, current, voltage | For building multilayer walls, increase the travel speed progressively to drop the heat accumulation, so that we can keep constant layer width. |
| Fereidoon Marefat et al. (2023) [31] | Creep-resistance steel and stainless steel & M12 (98%Ar-2%CO2) and M14 (96%Ar- | WAAM using pulse –gas metal arc welding (P-GMAW) | Wire feed speed, Travel speed | M14 gas was much better with both the materials providing spatter free deposition, removes lacks of fusion, increases weld dilution and leads to flat wall surfaces when compare to M12 gas. |

| | 3%CO2-1%O2) shielding gas | | | |
|---|---|---|---|---|
| Y.B. Liu et al. (2015) [32] | 5A06 aluminum alloy, AlSi5 (ER4043) filler wire | CMT | Welding current, welding velocity | As welding speed increases, IMC layer thickness first decreases and then increases. Thin thickness of IMC layer offers good shear strength and it decreases as the layer thickness increases. |
| Alfredo Suárez et al. (2022) [33] | Mild steel and stainless steel with ER70S-6 steel and 316L stainless steel wire | WAAM using GTAW and GMAW | Current, travel speed | Overlapping wall have more UTS and YS compared to sandwiched wall but is less ductile. No pores, micro-cracks or lack of fusion were found in the microstructure. |
| Xuewei Fang et al. (2018) [34] | 2219-T87 aluminum alloy | CMT | Arc mode, wire feed speed, travel speed | CMT-PADV arc mode was the most suitable mode for deposition of 2219 aluminum alloys, giving almost no larger pores, smallest pore area and pore aspect ratio and isotropic strength properties. |
| Peng He et al. (2022) [35] | ER6061 aluminum alloy | WAAM, CMT, FSP | Wire feed speed, welding speed | FSP increased the micro-hardness (by 31.5%), UTS (by 6%) and YS (by 23.3%), decrease porosity, anisotropy, and the elongation difference between horizontal and vertical directions. |
| Seung Hwan Lee (2020) [36] | AH36 steel, 316L stainless steel wire | WAAM, CMT, Gaussian Process Regression (GPR) | Wire feed rate, travel speed, Interpass time | Wire feed rate increases the surface waviness causes irregular weld and spattering. Travel speed causes unstable arc which results in irregular bead shape. Interpass time affects heat accumulation as bottom layer cooling rate is higher |

| | | | | as heat dissipates from substrate while cooling rate for top layer is low thus, heat accumulated and bead shape disturbs. Same results were obtained from GPR model and thus this model can be used for optimizing the parameters. |
|---|---|---|---|---|
| Guo-yin ZU et al. (2012) [37] | Steel panel and 5105 aluminum core | CMT | Panel thickness and core thickness | Bending load increases as thickness of panel and core was increased but there was not that much change in bending deflection. First there was shear failure of foam core and then delamination off the glued surface. Optimized thickness were 8 mm for panel and 50 mm for foam core. |
| Chen Zhanga et al. (2017) [38] | Al-6Mg aluminum alloy | CMT, CMT-P, VP-CMT | Arc mode, heat input, interlayer wait time, arc current, arc voltage | VP-CMT arc mode have the maximum UTS, equiaxed and refined grain size, improved mechanical properties compare to other arc mode. |
| N.T. Kumbhar et al. (2012) [39] | Al 5052, Al 6061 aluminum alloy | FSW | Tool rotation speed, tool traverse speed | Nugget section have sudden changes in hardness despite there was no rigorous mixing in both material. Tensile properties of weld were better than one of the soft material (Al 6061). |
| K. Vijaya Krishna Varma et al. (2021) [40] | Al 6082 aluminum alloy | FSW | Tool rotation speed, | With increase in tool rotation speed, excessive heat generation can be seen which causes circular onion rings, brittle product formation, tunnel defects, voids and cavities. All this can be eliminated by reducing the tool speed rotation. |

| Gurmeet Singha et al. (2017) [41] | Al 6082 aluminum alloy | FSW & TIG welding | (Tool rotation speed, Axial force, welding speed) for FSW & (Current) for TIG | More tensile strength and impact strength is achieved in case of FSW process compared to TIG process. |
|---|---|---|---|---|

## 2.1 Literature summary

In [7], authors tried to make a lap joint was welded using aluminium alloy and galvanized mild steel with the help of aluminium wire using CMT technology. Process parameters for the process were Wire-feed speed, Welding speed, Deviation distance, Voltage, Coating, Wire, Aluminum base metal. Taguchi Design of experiment was used to optimize these process parameters and ANOVA was used to find out the significance of each process parameters. On the basis of DoE and ANOVA, it was found out that the wire type is one of the most influential process parameter and thus Al4043 wire was selected to weld AA6061T6 base metal with mild steel sheet. After doing static testing, it was concluded that the strength of weld joint depends upon thickness of intermetallic layer and HAZ and can be controlled by controlling the heat input (increases with increase in heat input, after 200 J/mm it decreases).

In [8], authors tried to manufacture a weld in lap configuration using aluminum alloy (AA 2219) with stainless steel (AISI 321) using Friction stir welding and Cold Metal Transfer technology. Coating of aluminum has been deposited on stainless steel using friction stir welding. After that, using coating thickness as process parameter both materials have been joined in lap style. After investigation of the weld via SEM micrograph, Lap-shear test and Microstructure Analysis, it was concluded that as the aluminum interlayer coating thickness increases, intermetallic layer thickness decreases, thus increase in strength can be observed and poor wetting problem of liquid aluminum over steel was also overcome. And optimum interlayer aluminum thickness was found to be 0.6 mm, withstanding the highest tensile-shear load of 260 N/mm.

In [9], authors studied and compared the lap joint of two dissimilar material i.e., 5052 Al alloy and galvanized stainless steel which were fabricated by two process namely MIG

welding and CMT welding technique. Process parameters for the process were weld speed and wire feed rate. After comparing the two lap joints, it was concluded that though the Al-Fe-Si IMC layer formed by both the process, the layer was thick and Aluminum rich in MIG sample while it was thin and Iron rich in CMT sample.

In [10], authors studied the lap joint welding of two dissimilar material i.e., 6061-T6 aluminum alloy with zinc coated low carbon steel using ER4043 filler wire using CMT technique. Process parameters for the process were lap presetting gap and offset distance. Mechanical tests were carried out and it was concluded that weld strength increases as the lap presetting gap size increases and decreases by increases in off distance. As the gap was increased to some extent, zinc coating accumulates there which was stopping the intermetallic layer formation.

In [12], authors studied the mechanical properties of butt welded AA6082 aluminum alloy using FSW. Parameters for the process were Tool rotation speed, Traverse speed, and Axial force. From tensile, hardness test and microstructure analysis, it was concluded that weld region have fine grain structure compared to base metal region which have coarser grain. Nugget zone have the highest hardness value of 86.36 VHN and optimum value for best tensile strength were 1000 rpm tool rotation speed, axial force of 8 kN, and 2.5 mm/sec of traverse speed.

In [13], authors welded the AA6082 aluminum alloy using FSW with three different tool profiles (triangular, square, and hexagonal) and then compared the microstructure and mechanical properties of all of them. After all the experimentation work, it was found out that the specimen which was welded with hexagonal tool profile has the highest tensile strength among the three and the triangular profile welded specimen have the least strength. Also, hexagonal tool profile specimen have the uniformly distributed and smaller grain size compare to all other tool profile. Thus, it was concluded that as the number of sides of the tool profile increases, there is reduction in grain size in weld zone and thus increase in tensile strength is there.

In [21], authors investigated and compared the various modes of CMT arc characteristics i.e., CMT, CMT-P (pulse mode), CMT-VP (variable pulse mode) on 5A56 aluminum alloy.

Process parameters were Arc voltage and wire feed speed. After various microstructure and mechanical properties test, it was concluded that among the three arc modes, CMT-VP has better thermal management ability, lower heat input, construct fine equi-axed grains and smoother profile with having better mechanical properties compared to CMT and CMT-P mode.

In [26], authors tried to make a butt weld using low carbon thin sheets as a base material using Cold Metal Transfer and Metal Arc Gas welding and then compare the both. Process parameters were welding speed and weld bead width. After investigating the cross section and tensile tests on the weld, it was found that CMT is a better option for producing thin plates weld bead geometry and the welding speed has a direct influence on the weld bead profile and Heat affected zone (HAZ). High velocity can cause increase in reinforcement and thus gives improper penetration.

In [27], authors performed experiments to understand the stability of aluminum alloy forming by using the Cold Metal Transfer technology. For this, they have selected ER4043 as welding wire and 6061-T6 as base plate with process parameters being Wire feeding speed, Current, Voltage, and different arc mode. By analyzing different shape and structure of weld, it was concluded that the cross-section width and height can significantly affected by all the process parameters as well as shape feature (shape curvature). Increase in wire feeding speed as well as shape curvature can adversely affect the stability of the weld.

In [28], authors investigated the influence of arc length (single variable) on the weld bead geometry. For this, AISI 316L stainless steel was selected as base material and ER 308L was the filler wire. They used the Cold Metal Transfer technology to perform the weld for getting the lower heat input. After conducting the tensile and hardness test for the specimen, it was concluded that as the arc length correction increased, the top reinforcement and strength of weld, both increases. The strength of weld metal is 10.1% higher than the base metal due to presence of delta-ferrite in weld zone. 10% arc length correction was optimum for getting best weld.

In [29], authors investigated the effect of double side butt welding on the microstructure and mechanical properties b joining two dissimilar aluminum alloy materials using Cold Metal

16

Transfer technique. For this, the optimized process parameters were welding current, arc voltage, welding speed, wire feed speed, arc length correction, heat input. After investigation, it was concluded that by using CMT technique, the joint efficiency was better comparing to other welding process joining two dissimilar material. Also, weld zone was successfully obtained with an average hardness of $88 \pm 6$ HV.

In [30], authors investigated the effects of various process parameters (average power, travel speed, current, and voltage) on geometrical characteristics of an aluminum alloy. For this, the used the Cold Metal Transfer process to deposit the monolayer bead and add them upto 100 layer to make a wall. After the study, it was concluded that for building multilayer walls, we have to progressively increase the travel speed to drop the heat accumulation so that we can keep constant layer width.

In [31], authors tried to study the effect of shielding gas on the bi-metallic WAAM wall of two materials namely creep resistant steel (CRS) and stainless steel (SS) for improving process stability and build quality. The two shielding gasses were M12 (98%Ar-2%CO2) and M14 (96%Ar-3%CO2-1%O2) and process parameters were wire feed speed and travel speed. The technique used to create the bi-metallic WAAM wall was pulse-gas metal arc welding (P-GMAW). Arc stability and bead uniformity and penetration pattern were the major criterion to judge the appropriateness of the shielding gas. After investigation it was concluded that the M14 gas was much better with both the materials providing spatter free deposition, removes lacks of fusion, increases weld dilution and leads to flat wall surfaces when compare to M12 gas.

In [32], author studied the microstructure and mechanical properties of a 5A06 aluminum alloy lap jointed with an N6 pure Nickel plates using AlSi5 (ER4043) filler wire CMT technology. Welding speed was taken as process parameter for the process. An Intermetallic Compound (IMC) layer formation can be seen at the aluminum-nickel interface and after investigation, it was concluded that IMC layer thickness first decreases and then increases with increase in welding velocity while it's shear strength decreases as the IMC layer thickness increases i.e., minimum IMC layer thickness is required for having good shear strength.

In [33], authors fabricated a bi-metallic wall type structure with two materials i.e., mild steel and stainless steel by using GMAW and GTAW based WAAM technique in sandwich and overlapping strategies. Current and table speed were considered as process parameters for the process. After doing mechanical and microstructure analysis, it was concluded that the overlapping wall have more UTS and YS compared to sandwiched wall but is less ductile. Also, no pores, micro-cracks or lack of fusion were found in the microstructure.

In [34], authors investigated the effect of different types of arc mode on microstructure (porosity, pore size distribution, microstructure evolution) and mechanical properties of 2219 aluminum alloy using CMT technique. The different arc modes were CMT, CMT-P (pulse), CMT-ADV (advance), & CMT-PADV (pulse advance). Process parameters for the process were arc modes, wire feed speed, and travel speed. After all the tests, it was concluded that CMT-PADV arc mode was the most suitable mode for deposition of 2219 aluminum alloys, giving almost no larger pores, smallest pore area and pore aspect ratio and isotropic strength properties among all the arc modes.

In [35], authors compared the microstructure and mechanical properties before and after the post-treatment Friction Stir Processing process of an ER6061 aluminum alloy wall deposited by WAAM process. Process parameters that were used were wire feeding speed, and welding speed. First authors prepared the wall of the 6061 aluminum alloy by WAAM and after that compare all the properties of wall before and after by a post treatment process called Friction Stir Processing (FSP). After investigation, it was concluded that FSP significantly reduced the porosity, increased the micro-hardness (by 31.5%), UTS (by 6%) and YS (by 23.3%), decrease anisotropy and the elongation difference between horizontal and vertical directions.

In [36], authors optimized the CMT-WAAM process parameters using Gaussian Process Regression (GPR) model for improving quality and productivity of deposited shape using AH36 steel as substrate and 316L as feed wire. The optimized process parameters were Wire feed rate, Travel speed, and Interpass time. Experimental results showed three point. First, as the wire feed rate increases, surface waviness increases and weld becomes irregular, spattering occurs. Second, increase in travel speed causes unstable arc which results in irregular bead shape. Third, Interpass time affects heat accumulation as bottom layer cooling rate is higher as heat dissipates from substrate while cooling rate for top layer is low thus,

heat accumulated and bead shape disturbs. Same results were obtained from GPR model and thus this model can be used for optimizing the parameters.

In [37], authors conducted the three-point bending test on sandwich material having steel panel and aluminum 5105 alloy as core which were jointed with glue. The aluminum core was processed with CMT technique. Process parameters were panel and core thickness. After the three-point bending test, it was concluded that as the thickness of panel and core increases, maximum bending load also increases. First there was shear failure of foam core and then delamination off the glued surface. Optimized thickness were 8 mm for panel and 50 mm for foam core.

In [38], authors studied the various arc modes of CMT (CMT, CMT-P (pulse), CMT-VP (variable polarity)) for building an Al-6Mg aluminum alloy wall. Process parameters were arc mode, heat input, Interlayer wait time, arc voltage and arc current. After various microstructure and mechanical tests, it was concluded that the parts which were fabricated by VP-CMT arc mode have the maximum UTS, equi-axed and refined grain size, improved mechanical properties compare to other arc mode.

In [39], authors have performed the Friction Stir Welding of two dissimilar aluminum alloy (Al 5052 & Al 6061) in a butt configuration at different combinations of tool rotation speed and tool transverse speed and studied various microstructure and mechanical properties. After welding successfully, it was concluded that in nugget section, there was no rigorous mixing in both material but abrupt changes in the micro-hardness was seen across the nugget. The tensile properties of weld were better than one of the soft material (Al 6061).

In [40], authors study the effect of process parameter (tool rotation speed) and different geometric tool profile on AA6082 aluminum alloy butt joint welded using FSW technology. After conducting the experimental work, it was found out that as there is increase in tool rotation speed and transverse speed, there is excessive heat generation which causes altered circular onion rings, formation of brittle product, tunnel defects, voids, and cavities and all can be eliminated by reducing the tool rotation speed and choosing suitable process parameters.

In [41], authors studied the comparison of mechanical and microstructure properties of FSW process and TIG process for a butt jointed aluminum AA6082 alloy. Process parameters for FSW were tool rotation speed, axial force and welding speed while that for TIG was Current. After all the experimentation work, it was seen that the tensile strength of FSW specimen was nearly 85% more than the base metal while for TIG specimen, it was only 65% because in FSW weld region, there were equiaxed grain structure while in TIG specimen, there were coarser and elongated grain structure. Impact strength in case of FSW sample was double of base metal due to the stirring effect while in TIG sample, it was half. Micro-hardness were reduced in both the cases compared to base metal. Overall, FSW can be a better choice for welding aluminum alloy compared to TIG welding.

## 2.2 Research gap

On the basis of literature review, following research gaps have been observed:

1. Although there are various welding techniques such as TIG, FSW, etc. but it is still quite difficult to weld Aluminium alloy defect free due to more heat input, as Aluminium alloys are hard to weld materials,
2. CMT and FSP individually have been done in various researches, but effect of FSP over CMT butt welded specimen has not been found for the particular base material and filler wire.
3. Most of the published work focused on FSP over TIG or FSP over FSW, but there is still need to develop a process which minimizes defects and produce spatter free weld with upgraded mechanical and microstructure properties.

## 2.3 Objective of work

Aluminium is widely accepted in different types of industrial and construction work as it has lucrative properties over other material. New hybrid welding techniques have been continuously used for research purpose and they need to be used in industries as well. As a result, end results should be sound and efficient using hybrid techniques. By noticing the research gaps, the main goal of the study is to observe the mechanical and microstructure properties of a hybrid process and optimize the result to improve the weld. Following objectives were there for this study as shown below:

1. To form a sound weld using CMT process with the help of ER5356 filler wire and to do FSP over it,
2. To study the effect of process parameter for both the processes i.e., CMT as well as FSP over CMT process for good welded joints,
3. To optimize the process parameter for both the process to maximize UTS,
4. To watch the characterization and change in mechanical properties such as UTS, microhardness by doing FSP over CMT welded sample.

# CHAPTER 3

# EXPERIMENTAL WORK AND METHODOLOGY

## 3.1. Material selection

### 3.1.1 Aluminium AA6082

AA6082 is one of the member of aluminium 6000 series and has highest strength among fellow series mates. It is also known as structural alloy. Main constituents of AA6082 alloy are Silicon (0.7 – 1.3 %) & Manganese (0.4 – 1.0 %). Excellent machinability, weldability, resistance to corrosion are some of the properties of this alloy. Application area consists of rail coach parts, machine building and mobile cranes, offshore constructions, high stress applications like bridges, beer canes, cranes, etc. As it have a fine grain structure, this alloy exhibits a good resistance to dynamic loading conditions. The composition of the alloy is given in Table 3.1 and Table 3.2 for base metal and filler wire respectively.

### 3.1.2 ER5356

ER5356 is a magnesium rich alloy which is generally used in welding of aluminium 5000 series. It have high resistance to corrosion and have high relative shear strength. It shows good compatibility with the AA6082 aluminium alloy.

## 4.2 Composition:

Table 3.1 Chemical composition of parent material AA6082 as per ASTM standards

| Element name | Manganese (Mn) | Iron (Fe) | Magnesium (Mg) | Silicon (Si) | Copper (Cu) |
|---|---|---|---|---|---|
| Composition in % | 0.4 – 1.00 | 0.0 – 0.50 | 0.6 – 1.20 | 0.7 – 1.30 | 0.0 – 0.10 |
| Element name | Titanium (Ti) | Zinc (Zn) | Chromium (Cr) | Aluminium (Al) | |

| Composition in % | 0.0 – 0.10 | 0.0 – 0.20 | 0.0 – 0.25 | Remainder |
|---|---|---|---|---|

Table 3.2 Chemical composition of filler wire ER5356 as per ASTM standards

| Element name | Manganese (Mn) | Iron (Fe) | Magnesium (Mg) | Silicon (Si) | Copper (Cu) |
|---|---|---|---|---|---|
| Composition in % | 0.05 – 0.20 | 0.40 | 4.5 – 5.5 | 0.25 | 0.10 |
| Element name | Titanium (Ti) | Zinc (Zn) | Chromium (Cr) | Aluminium (Al) | |
| Composition in % | 0.06 – 0.20 | 0.10 | 0.05 – 0.20 | Remainder | |

## 4.3 Sample size and type of joint

Dimension of specimen of aluminium alloy AA6082 was 100x40x5 mm^3 and was produced by shearing machine. For performing butt joint, a 5xxx series aluminium alloy ER5356 filler wire material was used whose diameter was 1.2 mm. Total 18 plates were there and from that 9 butt joined were executed using CMT machine. FSP was done on the CMT welded butt joint up to half of the length i.e., 50 mm. for performing FSP, a non-consumable tool steel with 4 mm extruded pin tool was used which have length of 5 mm and shoulder diameter of 20 mm.

## 4.4 Development of CMT welding and FSP process

In the present study, two welding process has been implemented. First one is Cold Metal Transfer (CMT) while the other one is a hybrid process which is nothing but Friction Stir Processing (FSP) over CMT bead. CMT is a low heat input, spatter free process while FSP is a surface grain refinement process and can be used to eliminate porosity and surface defects by modifying the microstructure up to a certain depth. We have used ER5356 filler wire in butt joining the plates of AA6082 aluminium alloy using CMT process while no filler wire is needed in FSP hence it is an environment friendly process.

## 3.4.1. Selection of process parameters

Based on the previous literature reviews, it has been seen that process parameters like welding current, gas flow rate, and welding speed have prominent effect on the butt weld bead in CMT while tilt angle, table traverse speed, and tool rotation per minute affects the

quality of an FSP sample. Thus, these process parameters have been selected with different combinations in this study. Experiments were performed with different combinations of process parameters at factors and levels using Taguchi Design of Experiments method.

### 3.4.2    Design of Experiment

To make a relation between process input and process parameters output, a statistical tool "Design of Experiments" is used. It is widely accepted in different domains of medical science, engineering, and technology to maintain the relationship.

Designed by R. A. Fisher in the early part of $20^{th}$ century, it helps to manipulate different combinations of input, to find out their effect on a desired output. The purpose of DoE is to demonstrate the effect that a factor or independent variable has on dependent variable.

### 3.4.3    Taguchi orthogonal array design

It is a type of fractional orthogonal factorial design which is based on design matrix proposed by a Japanese engineer Genichi Taguchi. It has a two-level, three-level, and mixed-level design type. These orthogonal arrays are so balanced that it ensures that all level of all factors have been considered equally.

In this study, a three-level Taguchi design has been implemented with L9 runs so that it has 3 level design with 3 number of factors resulting in total 9 runs for the CMT process. While for the hybrid process, FSP over CMT, there was 2 level design with 3 number of factors resulting in total 9 runs. Fig. 3.1 shows the Taguchi design for various level in MiniTab.
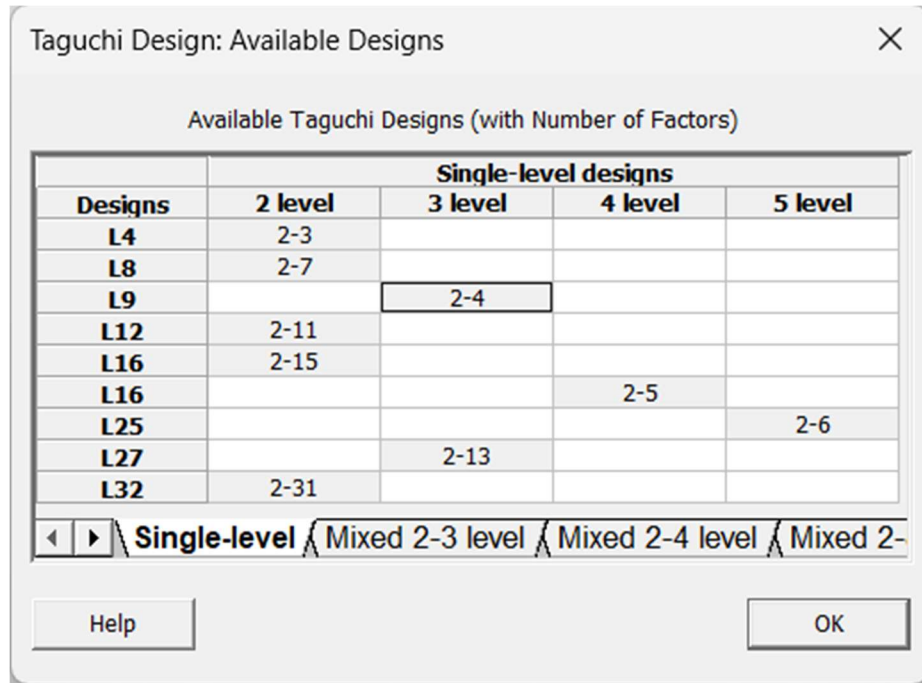
Figure 3.1. Taguchi design for various level in MiniTab

## 3.5 Experimental setup and Methodology

Various experiments were performed on the aluminium alloy table by changing one of the process parameter and keeping other unchanged. Different types of experiment were done according to Taguchi design table for both CMT process and FSP over CMT process. Parameter range were find out via two points. First, a general range were found out by doing literature review and after that, further range was found out by hit and trial method for different combination of process parameters.

Total 3 process parameters were taken for the CMT process which affects the quality of weld most. They were Welding current (WC), Welding speed (WS), and Gas flow rate (GFR). For FSP over CMT process, total two process parameters were taken by keeping the third parameter constant. The two process parameters were Tool rotation speed (TRS) and Table traverse speed (TTS). The parameter which was constant was the Tilt angle which was kept at 1° in clockwise direction. Table 3.3 shows the different operating range of the different process parameters that were used in this study for both the processes while Table 3.4 and Table 3.5 shows the orthogonal array for both the processes.

Table 3.3 Operating range of process parameters for both the processes

| CMT | | | | |
|---|---|---|---|---|
| **Symbols** | **Process parameter** | **Unit** | **Lower level** | **Higher level** |
| WC | Welding current | Ampere (A) | 170 | 190 |
| WS | Welding speed | cm/min | 35 | 45 |
| GFR | Gas flow rate | L/min | 12 | 18 |
| FSP over CMT | | | | |
| **Symbols** | **Process parameters** | **Unit** | **Lower level** | **Higher level** |
| TRS | Tool rotation speed | rpm | 700 | 1300 |
| TTS | Table traverse speed | mm/min | 40 | 80 |

Table 3.4 Orthogonal array for CMT process parameters

| S. No. | CMT | | |
|---|---|---|---|
| | **WC (A)** | **WS (cm/min)** | **GFR(L/min)** |
| 1 | 170 | 35 | 12 |
| 2 | 170 | 40 | 15 |
| 3 | 170 | 45 | 18 |
| 4 | 180 | 35 | 15 |
| 5 | 180 | 40 | 18 |
| 6 | 180 | 45 | 12 |
| 7 | 190 | 35 | 18 |
| 8 | 190 | 40 | 12 |
| 9 | 190 | 45 | 15 |

Table 3.5 Orthogonal array for FSP over CMT process parameters

| S. No. | FSP over CMT | | | | |
|---|---|---|---|---|---|
| | **WC (A)** | **WS (cm/min)** | **GFR(L/min)** | **TTS (mm/min)** | **TRS (rpm)** |
| 1 | 170 | 35 | 12 | 80 | 1300 |
| 2 | 170 | 40 | 15 | 80 | 1000 |
| 3 | 170 | 45 | 18 | 80 | 700 |
| 4 | 180 | 35 | 15 | 60 | 1300 |
| 5 | 180 | 40 | 18 | 60 | 1000 |
| 6 | 180 | 45 | 12 | 60 | 700 |
| 7 | 190 | 35 | 18 | 40 | 1300 |

| 8 | 190 | 40 | 12 | 40 | 1000 |
| 9 | 190 | 45 | 15 | 40 | 700 |

In this research experiment, butt weld were performed using CMT machines on 6xxx series aluminium alloy AA6082 of dimension 100x40x5 mm^3 using 5xxx series aluminium alloy ER5356 (Mg rich) filler wire of diameter 1.2 mm. The gap between the two aluminium plates were negligible. The machine that was used for performing CMT welds was TPS400i (developed by Fronius) which was connected by a robotic torch traveller to get a uniform welding speed and was controlled by a CMT machine controller as shown in Fig 3.2. CMT weld was done in the CMT-P (pulse) mode. 99.99% pure argon was used for the process.

Before performing the welding experiment, all the specimens were first cleared with acetone so that their will not be any accumulation of foreign particle or any oxide layer. After that, two plates were placed with negligible gap within them and were clamped and welded up to their full length. Welds were done with varying one process parameter and keeping other process parameter constant. Electrode and workpiece were perpendicular to each other and nozzle tip was 15 mm away from the specimen. Total 9 butt welded were performed for the experiment using 18 plates. The CMT machine was kept at Central Workshop, DTU and all the experiments were performed there only.
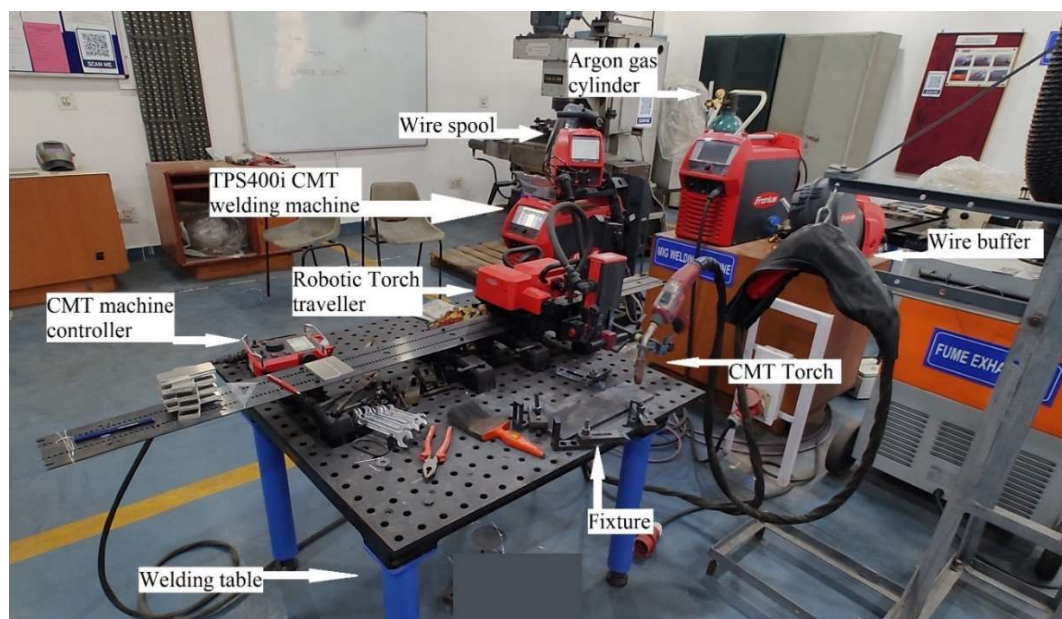


Figure 3.2. CMT machine, Central workshop, DTU

After that, FSP was done on the samples. The machine which was used for performing experiments was Friction Stir Welding (FSW) machine as shown in Fig. 3.3 on this machine, the CMT welded plate was kept in a base plate fixture and was hold by using hydraulic clamping. Using this machine, FSP was done in a straight line with single pass by considering TRS & TTS as process parameter and with constant 1° machine tilt angle in clockwise direction. The tool that was used for performing FSP was made from tool steel having shoulder diameter as 20 mm, extruded pin length as 4 mm, and pin diameter as 5 mm as shown in Fig. 3.4. The extruded tool pin has a cylindrical tool profile which was selected by doing various literature review. The FSP was done on the CMT welded samples up to half of its length i.e., 50 mm so that a comparative study can also be established. After FSP was done, its wavy chips were removed with the help of a grinder. The shown FSP machine was also in Central workshop, DTU and all the experiments were performed on there only.
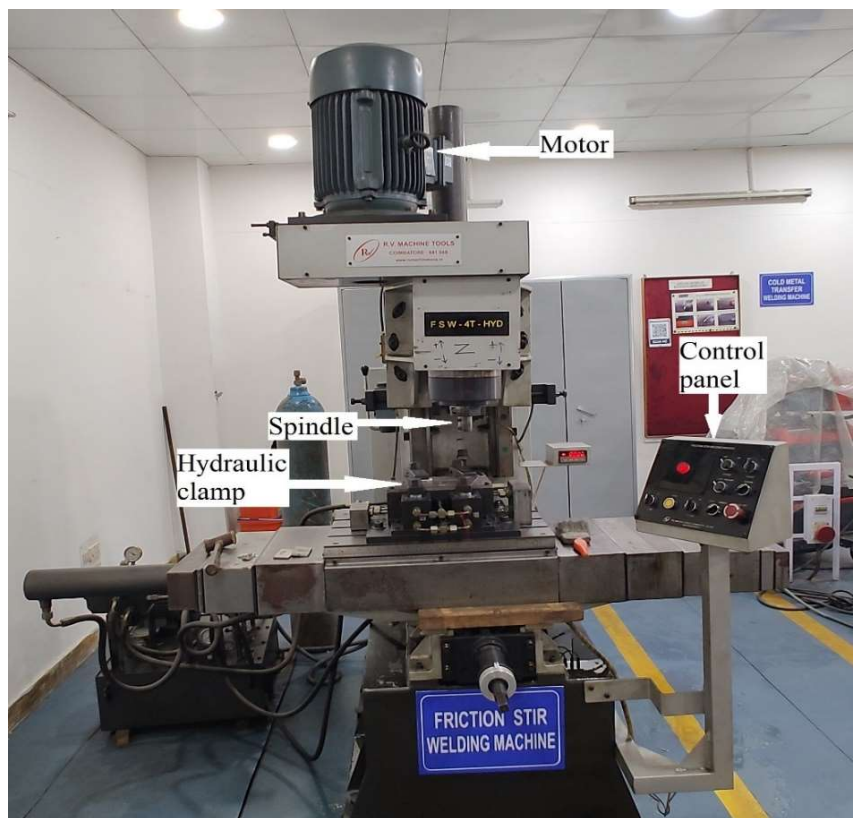


Figure 3.3. FSW/FSP machine, Central workshop, DTU

Figure 3.4. FSP tool

After the FSP, the butt joint plate consist of two different processes over it. Half of the plate was butt welded by using CMT, while half of the plate was butt welded by hybrid process i.e., FSP over CMT as shown in Fig. 3.5 all the samples were extracted from these welded plates only.
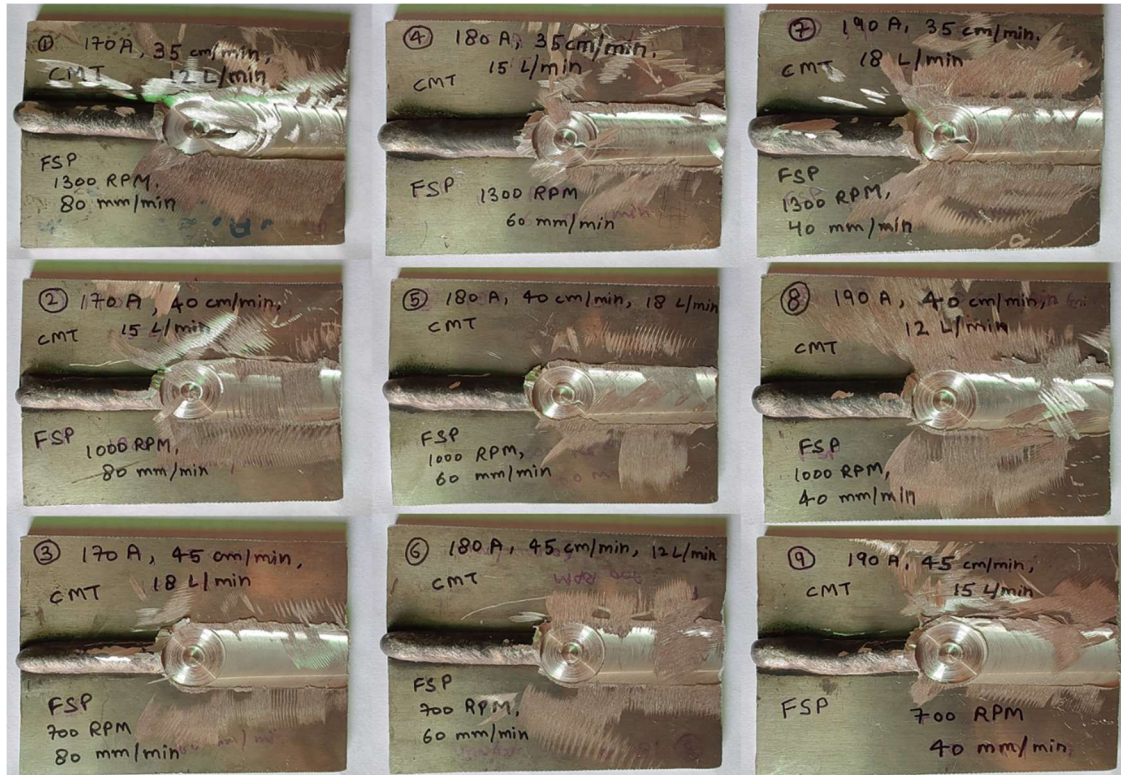


Figure 3.5. All butt welded specimens using two different processes

## 3.6 Characterization of welded joint

### 3.6.1 Tensile test

Tensile test were conducted for both the processes for understanding the behaviour of alloy AA6082 under tension load. For performing tensile test, an ASTM standard sample is tugged between the grippers of an UTM machine. All the samples were drawn out perpendicular to the weld line using wire EDM. Applied force and elongation value are calculated throughout the test at different points, and are there in the form of stress and strain. For tensile test, 18 ASTM E8 standard specimen has been cut using wire EDM machine. 9 samples for the tensile test of CMT process and 9 samples for the tensile test of FSP over CMT process shown in Fig. 3.6. ASTM E8 standard specimen has been shown in Fig. 3.7. All the samples were grooved manually so that there will be no slipping effect during tensile test. Two sample (B1 & B2) were drawn out from the base metal to understand the tensile property of base metal.
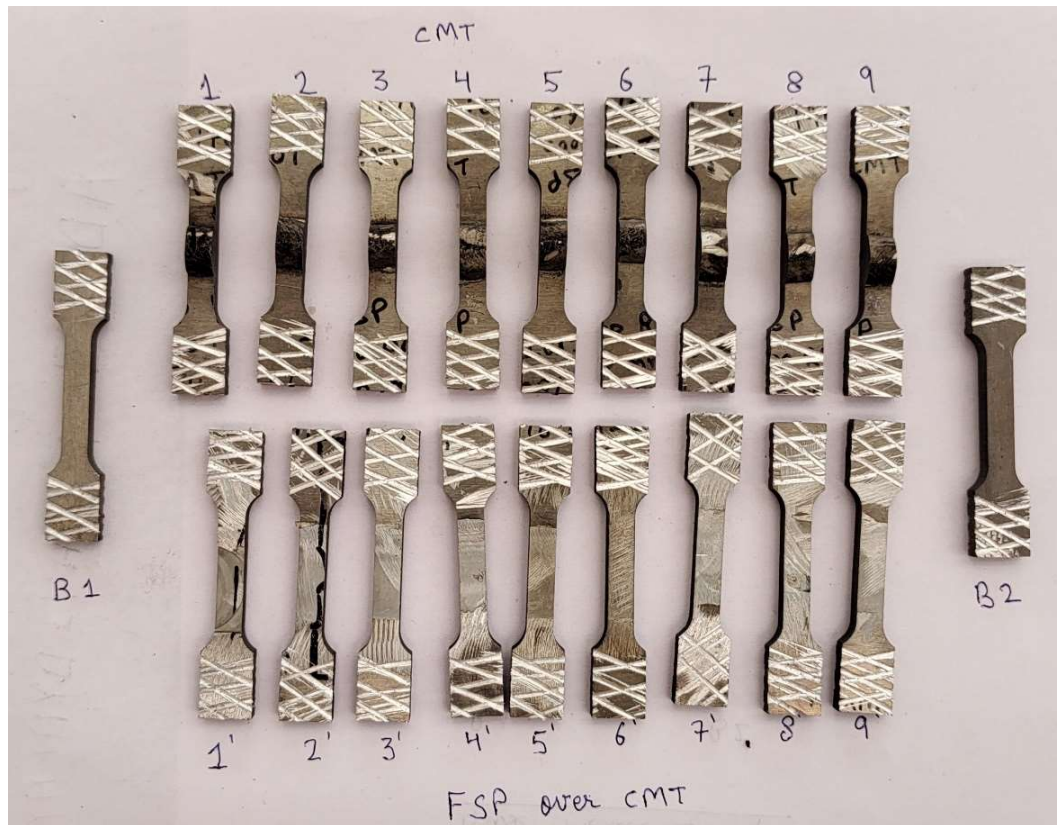


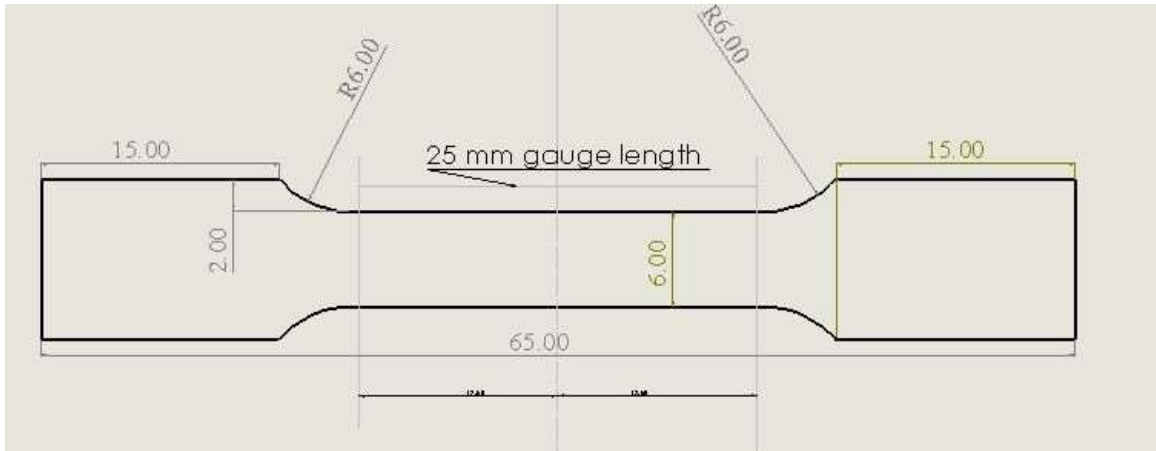Figure 3.6. All grooved samples for tensile test

Figure 3.7. ASTM E8 standard specimen

For conducting the tensile test, Universal Testing Machine (AI-UTM-T40) machine of 50 kN capacity was used as shown in Fig. 3.8. Cross-head velocity of 2.5 mm/sec was taken for each of the sample. Tensile test on the specimen was performed unit it cracks during pulling process.



Figure 3.8. UTM, Metal forming lab, DTU

Before and after tensile test of the samples are shown in Fig. 3.9 and Fig. 3.10 for CMT process and FSP over CMT process respectively. Ultimate Tensile Strength value obtained by UTS machine for CMT and FSP with CMT process are shown in Table 3.6 and Table 3.7.

Figure 3.9. CMT samples before and after tensile test

Table 3.6. UTS of CMT samples under different process parameters

| S. No. | CMT | | | |
|---|---|---|---|---|
| | WC (A) | WS (cm/min) | GFR (L/min) | UTS (MPa) |
| 1 | 170 | 35 | 12 | 116 |
| 2 | 170 | 40 | 15 | 122 |
| 3 | 170 | 45 | 18 | 89.1 |
| 4 | 180 | 35 | 15 | 149 |
| 5 | 180 | 40 | 18 | 169 |
| 6 | 180 | 45 | 12 | 103 |
| 7 | 190 | 35 | 18 | 173 |
| 8 | 190 | 40 | 12 | 180 |
| 9 | 190 | 45 | 15 | 192 |

Figure 3.10. FSP over CMT samples before and after tensile test

Table 3.7. UTS of FSP over CMT samples under different process parameters

| S. No. | FSP over CMT | | | | | |
|--------|--------|--------|--------|--------|--------|--------|
| | WC (A) | WS (cm/min) | GFR (L/min) | TTS (mm/min) | TRS (rpm) | UTS |
| 1 | 170 | 35 | 12 | 80 | 1300 | 133 |
| 2 | 170 | 40 | 15 | 80 | 1000 | 167 |
| 3 | 170 | 45 | 18 | 80 | 700 | 168 |
| 4 | 180 | 35 | 15 | 60 | 1300 | 88.8 |
| 5 | 180 | 40 | 18 | 60 | 1000 | 164 |
| 6 | 180 | 45 | 12 | 60 | 700 | 162 |
| 7 | 190 | 35 | 18 | 40 | 1300 | 155 |
| 8 | 190 | 40 | 12 | 40 | 1000 | 160 |
| 9 | 190 | 45 | 15 | 40 | 700 | 162 |

### 3.6.2 Optical Microscopy

To get the idea about the microstructure, grain boundary, and change in structure at the joint junction, heat affected zone of weld bead and parent material during welding, we do Optical microscope analysis. Following steps were involved in the preparation and analysis of the microstructure.

- A 10x15x5 mm^3 size samples were drawn from the butt welded specimen using wire EDM. Total 18 samples were taken out (9 for CMT and 9 for FSP over CMT) shown in Fig. 3.11.
- Cylindrical mould was created and samples were kept at bottom with weld raw surface downside, mixture of adhesive and resins was mixed and poured in it and left for solidification.
- Now polishing of the samples were done using emery paper starting from grade 200 to 2600.
- Finally, wet polishing was performed to get the mirror like surface finish as shown in Fig. 3.12.
- For observing the microstructure, samples were dipped in Keller's reagent with an ideal time of 10 sec.
- Finally, OLYMPUS LG-PS2 microscope was used to study the morphology of the weld bead samples (shown in Fig. 3.13).
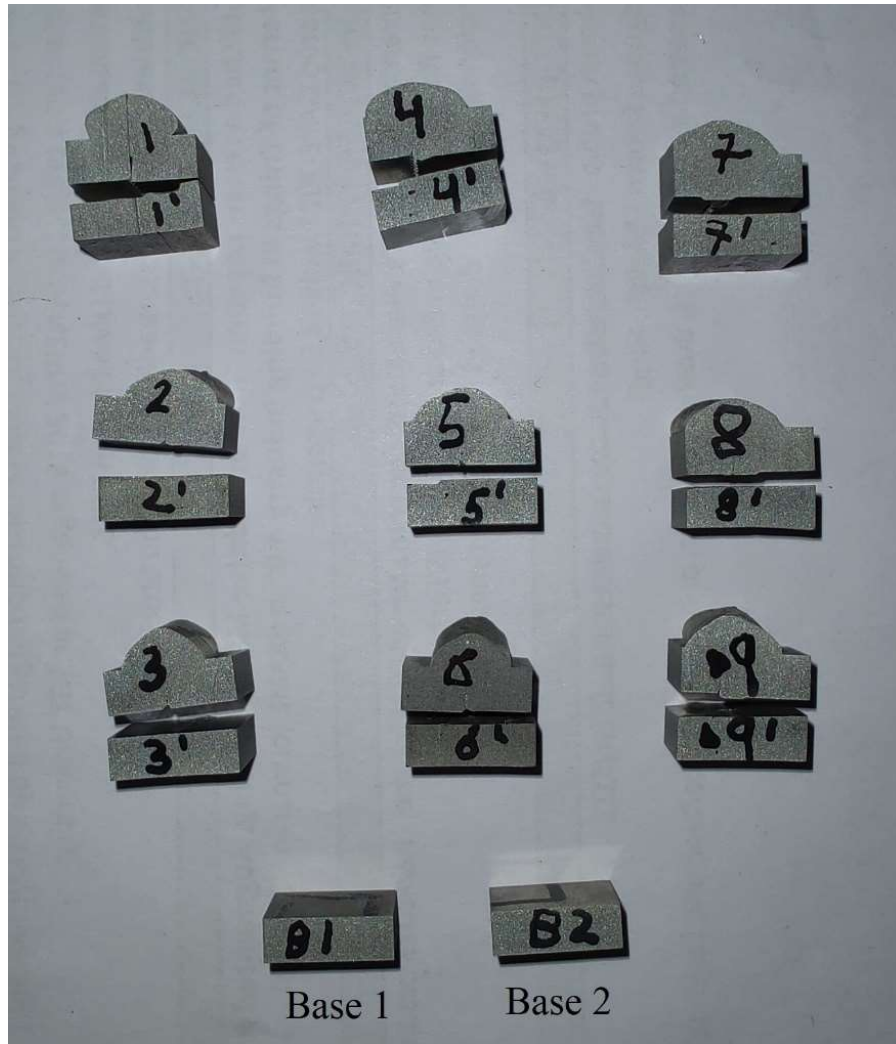
Figure 3.11 Samples before mounting

Specimens which have the highest tensile strength for both the processes were selected for the microstructure study. Hence, total 6 samples were selected (best 3 from CMT and best 3 from FSP over CMT) out of 18 samples. Analysis was done on the Heat Affected Zone (HAZ), Fusion Zone (FZ), and Base Metal (BM) for CMT welded specimen and while it was done on Sir Zone (SZ), and Thermo-Mechanical Affected Zone (TMAZ) for FSP over CMT specimen.
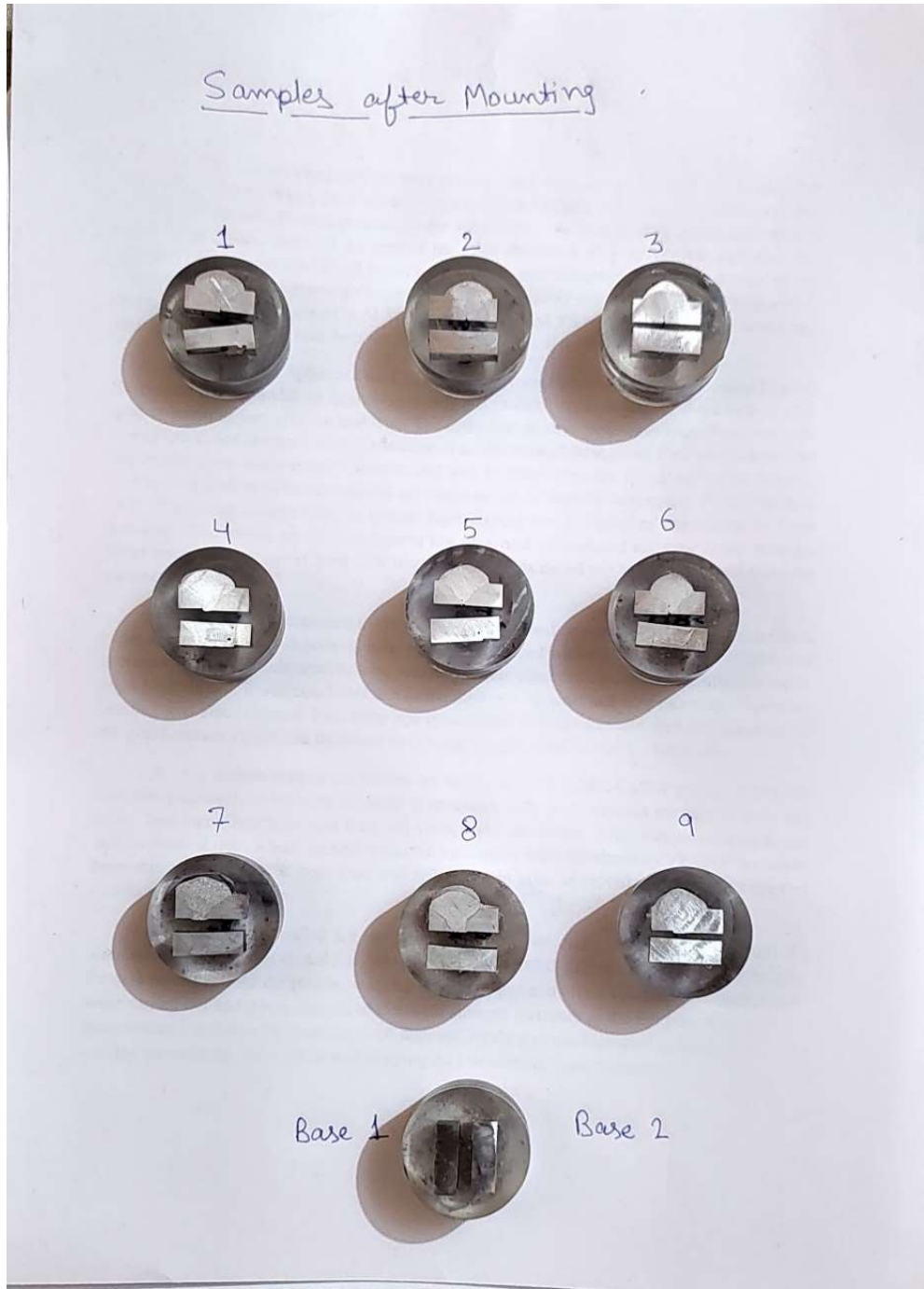
Figure 3.12 Samples after mounting

Figure 3.13 OLYMPUS LG-PS2 microscope, Metallurgy Lab, DTU

### 3.6.3   Microhardness analysis

Samples on which microstructure analysis were done, same samples were used to check their microhardness. This technique is used to determine the hardness of a material on a small scale. In this, load ranging from few grams to kilograms is applied on material with the help of a diamond indenter up to some dwell time. Then, by calculating the microscopic impressed diagonals dimension of the indentation as shown in Fig. 3.14, we find the hardness value of the specimen. Obtained hardness value tells us about the material's predicted service life and its characteristics.
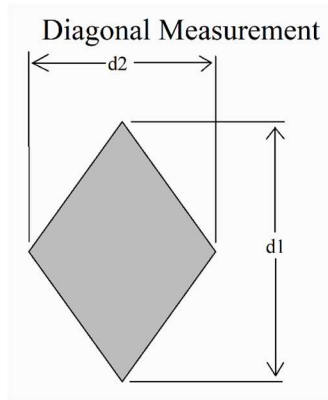
Figure 3.14 Pyramid shape indenter by Vickers hardness testing machine

For conducting the Vickers hardness test, DRAMIN-40 STRUERS microhardness tester was employed as shown in Fig. 3.15. The test was performed at a load of 500 gram for a dwelling period of 10 sec. The load and the dwelling period were selected by studying various literature on the same. Hardness values were taken at HAZ, FZ, & BM for the CMT samples and at SZ & TMAZ for FSP over CMT samples. Graphs were plotted for different zone hardness at different regions for both the processes.



Figure 3.15 DRAMIN-40 STRUERS microhardness tester, Metal Forming lab, DTU

# CHAPTER 4

# RESULT AND DISCUSSION

Aluminium AA6082 alloy has been welded in butt configuration by two methods. First was CMT welding process and second was FSP over CMT weld bead process. Main focus of this study was to find out the effect of FSP over the CMT samples and optimized process parameters for both the processes. To know about the microstructure and mechanical properties of the samples, tensile test, microstructure analysis, and hardness test was also performed.

## 4.1 Optimization using Taguchi technique

Minitab software was used to perform the Taguchi DoE table and ANOVA analysis. Minitab helps to get the desired results and its features helps to understand the relationship between output and input due to its friendly and logical interface.

The present research is using Taguchi technique and ANOVA so that meaningful results and relationships could be established between input parameters values and output values. For both the processes used for the research, experiments were performed using Taguchi L9 Orthogonal array since it helps to reduce the number of attempts of test, otherwise long experimental work had to be done. A 3-level (Welding current, Welding speed, Gas flow rate) with 3-factor orthogonal array was created for CMT welding process (Table 4.1) and 2-level (Table traverse speed, Tool rotation speed) with 3-factor was created for the FSP over CMT welding process (Table 4.2). Ultimate tensile strength was taken as a response variable for each of the welded joint. Larger value of S/N ratio characteristics was considered better for Taguchi method. Influence of process parameter on the weld joint were given respective rank.

Table 4.1 Orthogonal array for UTS of CMT welded joints

| S. No. | CMT | | | |
|--------|---------|-------------|-------------|-----------|
| | WC (A) | WS (cm/min) | GFR (L/min) | UTS (MPa) |
| 1 | 170 | 35 | 12 | 116 |
| 2 | 170 | 40 | 15 | 122 |
| 3 | 170 | 45 | 18 | 89.1 |
| 4 | 180 | 35 | 15 | 149 |
| 5 | 180 | 40 | 18 | 169 |
| 6 | 180 | 45 | 12 | 103 |
| 7 | 190 | 35 | 18 | 173 |
| 8 | 190 | 40 | 12 | 180 |
| 9 | 190 | 45 | 15 | 192 |

Table 4.2 Orthogonal array for UTS of FSP over CMT welded joints

| S. No. | FSP over CMT | | | | | |
|--------|---------|---------------|---------------|-----------------|--------------|------|
| | WC (A) | WS (cm/min) | GFR (L/min) | TTS (mm/min) | TRS (rpm) | UTS |
| 1 | 170 | 35 | 12 | 80 | 1300 | 133 |
| 2 | 170 | 40 | 15 | 80 | 1000 | 167 |
| 3 | 170 | 45 | 18 | 80 | 700 | 168 |
| 4 | 180 | 35 | 15 | 60 | 1300 | 88.8 |
| 5 | 180 | 40 | 18 | 60 | 1000 | 164 |
| 6 | 180 | 45 | 12 | 60 | 700 | 162 |
| 7 | 190 | 35 | 18 | 40 | 1300 | 155 |
| 8 | 190 | 40 | 12 | 40 | 1000 | 160 |
| 9 | 190 | 45 | 15 | 40 | 700 | 162 |

## 4.1.1 Analysis of Variance (ANOVA)

Analysis of Variance (ANOVA) was applied in this present research to find out the influence rank and percentage contribution of the individual process parameter on the response i.e., Ultimate Tensile Strength. ANOVA tells us that which parameter is more statistically significant. ANOVA table has been generated for both types of welding processes samples.

### 4.1.1.1 Optimization of weld specimen using CMT

By using Taguchi optimization method, we get our optimized process parameters for the CMT welding process. A larger value of Signal-to-Noise ratio was selected since we have to

find those optimized process parameters which increases our response i.e., UTS. Optimized process parameters are 190 A for the WC, 40 cm/min for the WS, and 15 L/min for the GFR.

The graph of main effect plot for SN ration is shown in Fig. 4.1 and response table for Signal-to-Noise ratio is shown in Table 4.3.
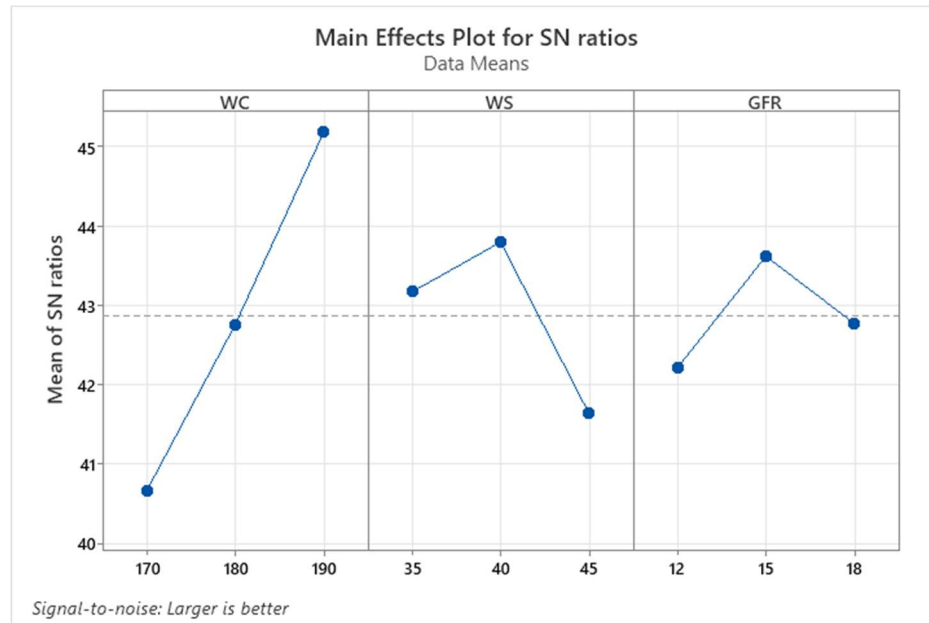


Figure 4.1 Main effect plot for SN ratio for CMT process

Table 4.3 Response table for SN ratio for CMT process

| Level | WC | WS | GFR |
|-------|-------|-------|-------|
| 1 | 40.67 | 43.17 | 42.22 |
| 2 | 42.76 | 43.80 | 43.62 |
| 3 | 45.18 | 41.64 | 42.77 |
| Delta | 4.51 | 2.16 | 1.40 |
| Rank | 1 | 2 | 3 |

ANOVA of SN ratio was used to find out the percentage of contribution of the individual parameter on the response characteristics i.e., UTS. Percentage contribution value were found out from the sequential square value given in the ANOVA of SN ration table. Percentage contribution was found out by dividing individual sequential square value by total value. From that, it is found that WC has maximum contribution (67.47%) on the UTS, WS has medium (16.33%) contribution on UTS, and GFR has minimum contribution (6.61%) on

UTS. Moreover, it can be seen that WC is proportion to UTS i.e., as the value of WC increases, UTS increases while in case of WS & GFR, it is not true. It is clear that WC has maximum effect on the UTS of the sample followed by WS and GFR. Percentage contribution of process parameters along with their sequential square value are shown in tabular form in ANOVA for SN ratios Table 4.4 below.

Table 4.4. ANOVA for SN ratio for CMT process

| Source | DF | Seq. SS | Percentage contribution |
|--------|----|---------| ------------------------|
| WC     | 2  | 30.513  | 67.47 |
| WS     | 2  | 7.387   | 16.33 |
| GFR    | 2  | 2.990   | 6.61  |
| Error  | 2  | 4.331   |       |
| Total  | 8  | 45.222  |       |

Table 4.5. Model summary for CMT process

| S | R-sq | R-sq (adj) |
|---|------|------------|
| 1.4716 | 90.42% | 61.69% |

The highest UTS found in CMT welded case was 192 MPa which was 75.88% of the BM. Prediction of response was also done by using the optimized process parameters value in the Taguchi prediction method. By using the WC 190 A, WS 40 cm/min, and GFR 15 L/min, predicted value of the response i.e., UTS was coming to be 205.64 MPa which was 81.28% of the base material and is showing an increment of 7.1% from the highest value of UTS. Table 4.5 shows the model summary. The R-sq value in the model summary shows that the model is 90.42% of the variance in the strength.

**4.1.1.2 Optimization of weld specimen using FSP over CMT**

By using Taguchi optimization method, we get our optimized process parameters for the FSP over CMT welding process. A larger value of Signal-to-Noise ratio was selected (same as of CMT process) since we have to find those optimized process parameters which increases our response i.e., UTS. Optimized process parameters are 40 mm/min for the TTS, and 700 rpm for the TRS.

The graph of main effect plot for SN ration is shown in Fig. 4.2 and response table for Signal-to-Noise ratio is shown in Table 4.6.
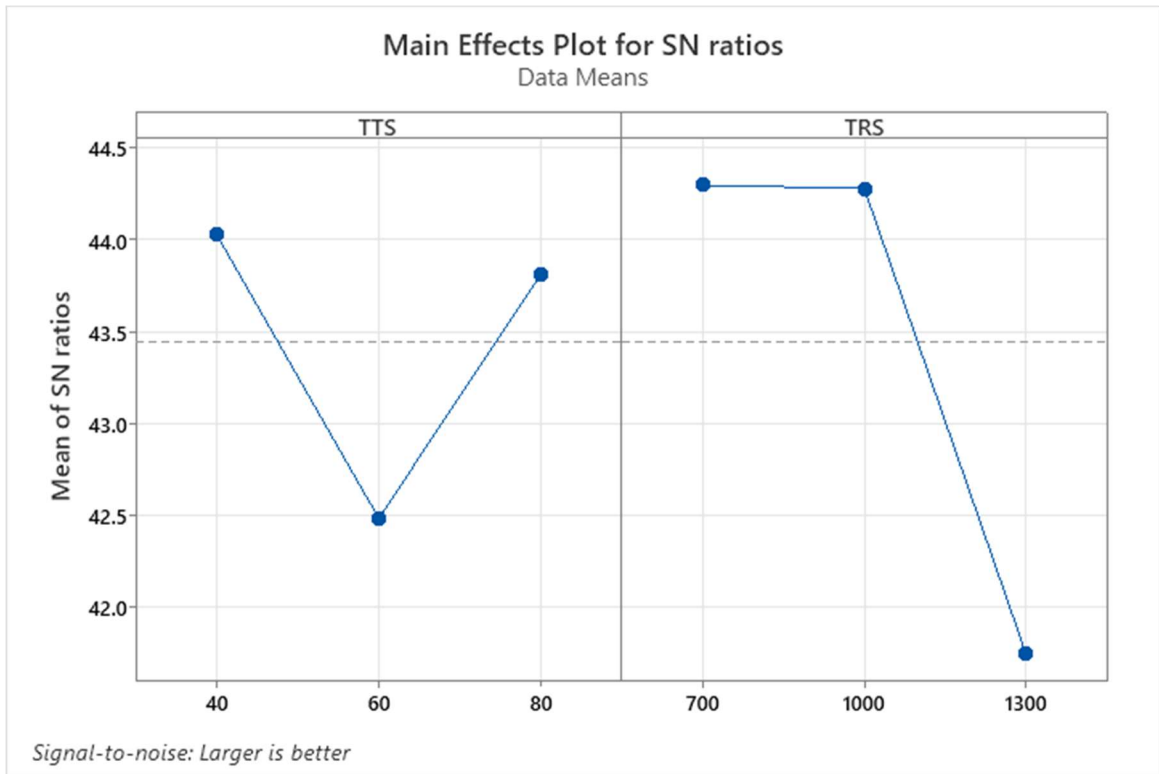


Figure 4.2 Main effect plot for SN ratio for FSP over CMT process

Table 4.6 Response table for SN ratio for FSP over CMT process

| Level | TTS | TRS |
|-------|-------|-------|
| 1 | 44.03 | 44.30 |
| 2 | 42.49 | 44.28 |
| 3 | 43.81 | 41.75 |
| Delta | 1.54 | 2.54 |
| Rank | 2 | 1 |

ANOVA of SN ratio was used to find out the percentage of contribution of the individual parameter on the response characteristics i.e., UTS. It is found that TTS has minimum contribution (16.40%) on the UTS, on the other hand TRS has maximum contribution (50.45%) on UTS. It is noticeable that as the TRS changes from 700 rpm to 1000 rpm, there is not much effect on the UTS, but as the TRS changes from 1000 rpm to 1300 rpm, UTS

decreases rapidly. This is due to the fact that samples over which FSP was done taking TRS as highest (1300 rpm), tunnel defects were seen due to which UTS decreases. At higher TRS more heat generation will be there and thus generation of tunnel defect occurs [39]. It can be seen clearly that TRS has more effect on the UTS of the sample followed by TTS. Percentage contribution of process parameters along with their sequential square value are shown in tabular form in ANOVA for SN ratios Table 4.7 below.

Table 4.7 ANOVA for SN ratio for FSP over CMT process

| Source | DF | Seq. SS | Percentage contribution |
|--------|----|---------|-------------------------|
| TTS | 2 | 4.183 | 16.40 |
| TRS | 2 | 12.864 | 50.45 |
| Error | 4 | 8.449 | |
| Total | 8 | 25.497 | |

Table 4.8 Model summary for FSP over CMT process

| S | R-sq | R-sq (adj) |
|---|------|-----------|
| 1.4534 | 66.86% | 33.72% |

Highest UTS in case of FSP over CMT welded samples was 168 MPa which was 66.40% of BM. Prediction of response was also done by using the optimized process parameters value in the Taguchi prediction method. By using the TTS 40 mm/min and TRS 700 rpm, predicted value of the response i.e., UTS was coming to be 171.911 MPa which was 67.94% of the base material and is showing an increment of 2.3% from the highest value of UTS. Table 4.8 shows the model summary. The R-sq value in the model summary shows that the model is 66.86% of the variance in the strength.

From the Taguchi optimization technique and ANOVA method, it can be seen that for CMT welding process, Welding current is the most prominent process parameter for obtaining higher value of Ultimate Tensile Strength while in case of FSP over CMT welding process, Tool Rotation Speed is more prominent for obtaining higher value of UTS.

## 4.2    Tensile test

Tensile test were performed for all the welded joint specimens to find out their Ultimate Tensile Strength. Total 18 tests were performed (9 for CMT and 9 for FSP over CMT) and they all cut were in ASTM E8 standard.

Before conducting the tensile test for all the samples, 2 samples were drawn out in ASTM E8 standard from the base plate to check the UTS of the base plate. The average of the UTS of both the samples were 253 MPa. Grooves were made on these samples also so that slipping condition can be avoided and doesn't affect the results. Base plate samples before and after tensile test were shown in Fig. 4.3.
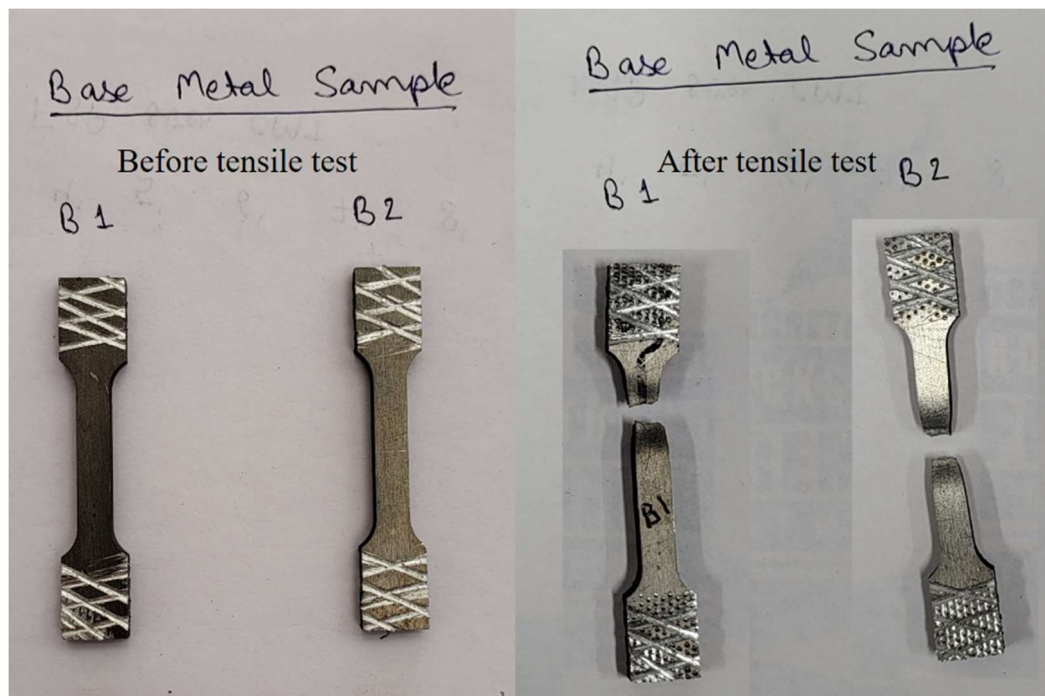


Figure 4.3 Base metal sample before and after tensile test.

## 4.2.1    Tensile test of CMT samples

All the 9 samples of welded joint were undergone the tensile test. From all the samples, some of them failed from welded zone (WZ), some failed from heat affected zone (HAZ), and some from base metal (BM) as shown in Fig. 4.4.
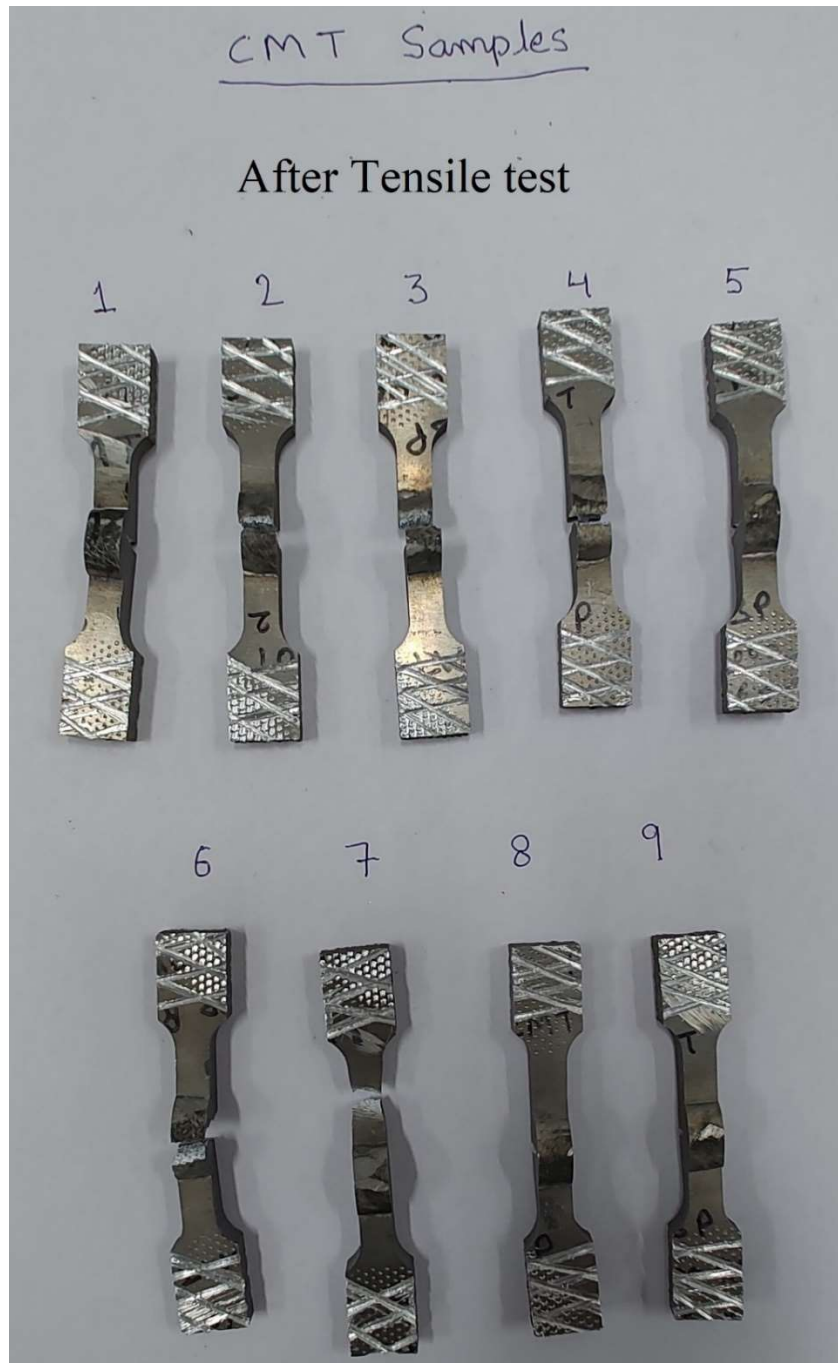
Figure 4.4 CMT samples after tensile test

Maximum ultimate tensile strength comes out from sample was 192 MPa for the sample number 9, when alloy AA6082 was welded using ER5356 filler wire in butt configuration having process parameter as 190 A WC, 45 cm/min WS, and 15 L/min GFR. The highest UTS is 75.88% of the BM while joint strength were found out to be 67% in previous studies

[41]. While it can be shown in Table 4.1 that sample number 7, 8, and 9, all three have been welded by taking 190 A WC and have the highest UTS among the 9 sample irrespective of WS and GFR. Stress strain diagram for sample number 9 has been shown in fig. 4.5 and comparative value of all the sample's UTS are shown in fig. 4.6. Also, Taguchi optimization was also pointing towards WC as a main contributor for the UTS. This shows that WC have more impact on the UTS and higher WC is recommended for getting higher UTS.
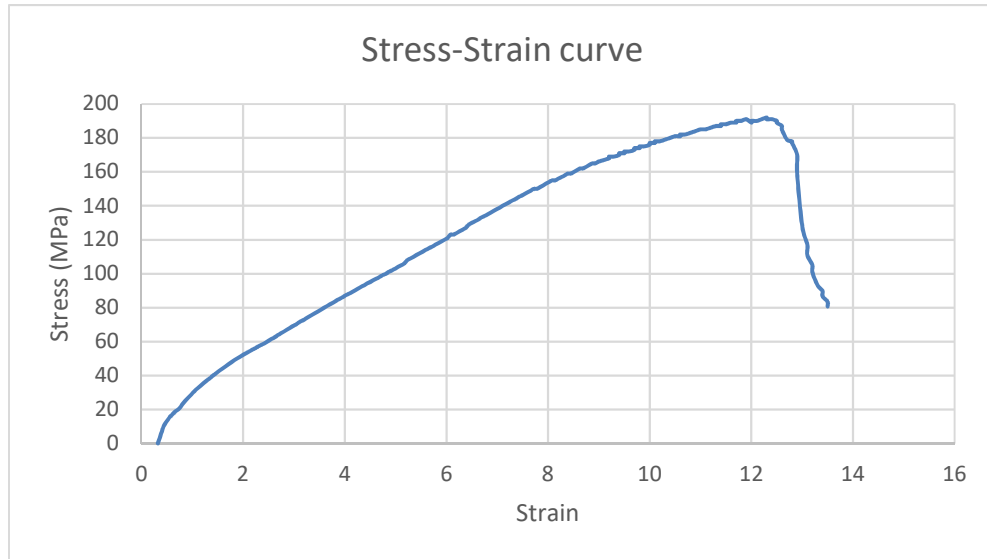


Figure 4.5 Stress strain diagram for 9th CMT welded sample
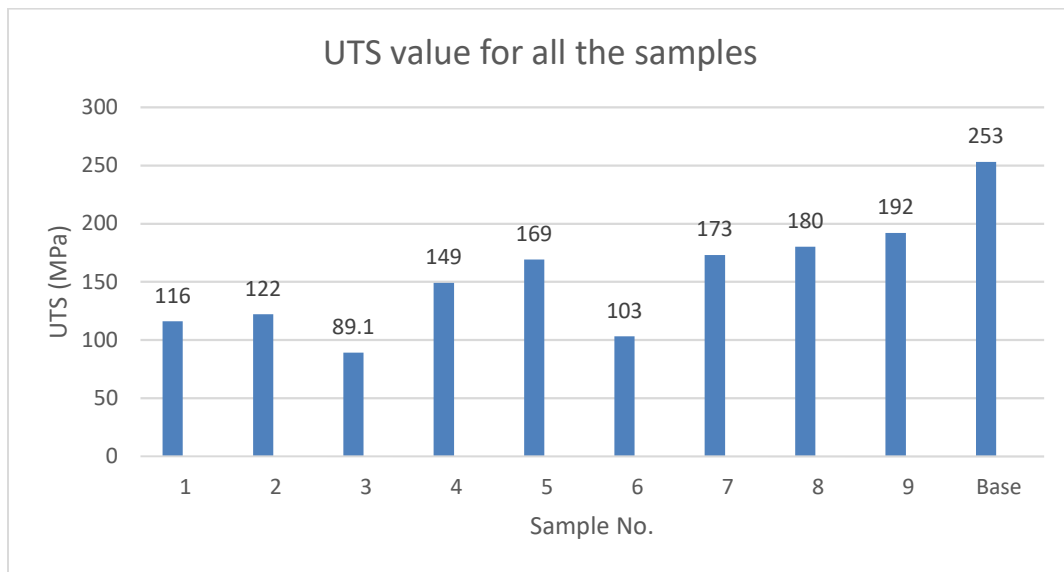


Figure 4.6 UTS value for all the CMT welded samples

### 4.2.2    Tensile test of FSP over CMT

All the 9 samples of welded joint were undergone the tensile test. From all the samples, some of them failed from nugget zone (NZ), some failed from heat affected zone/thermo-mechanical affected zone (HAZ/TMAZ), and some from base metal (BM) as shown in Fig. 4.7.

Maximum ultimate tensile strength comes out from sample was 168 MPa for the sample number 3, when alloy AA6082 was welded using ER5356 filler wire in butt configuration and over it FSP was done having process parameter as 170 A WC, 45 cm/min WS, and 18 L/min GFR for CMT process and 80 mm/min TTS and 700 rpm TRS for FSP process over it. The highest UTS is 66.40% of the BM while previous studies shows the joint strength of about 75 – 80% [42], 69% [43] of the BM. While it can be shown in Table that sample number 1, 2, and 3, all three have been welded by taking 170 A WC and 80 mm/min TTS have the highest UTS among the 9 sample (except sample 1) irrespective of WS and GFR. It can be also noted that sample number 2, 3, 5, 6, 8, and 9, all have equivalent UTS in range of 160 – 168 MPa. On the left out samples, FSP was done with maximum TRS of 1300 rpm. This concluded that a higher value of TRS is not much suitable for getting higher value of UTS. Also, as TRS is increases, UTS decreases for the same value of TTS [37].
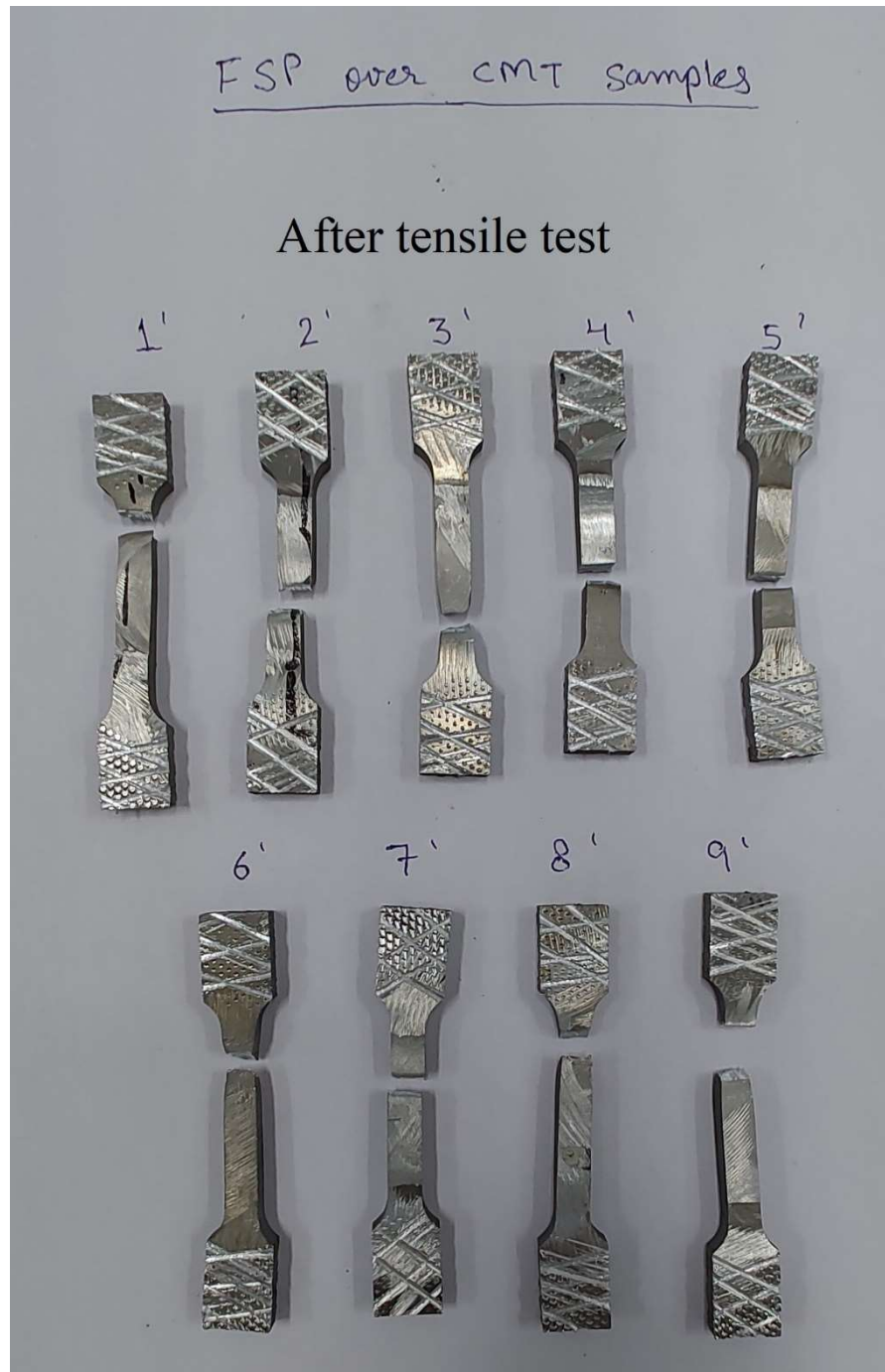
Figure 4.7 FSP over CMT samples after tensile test

Stress strain diagram for sample number 3 has been shown in fig. 4.8 and comparative value of all the sample's UTS are shown in fig. 4.9. Also, Taguchi optimization was also pointing towards TRS as a main contributor for the UTS which can be justified. This shows that TRS have more impact on the UTS and lower TRS is recommended for getting higher UTS.
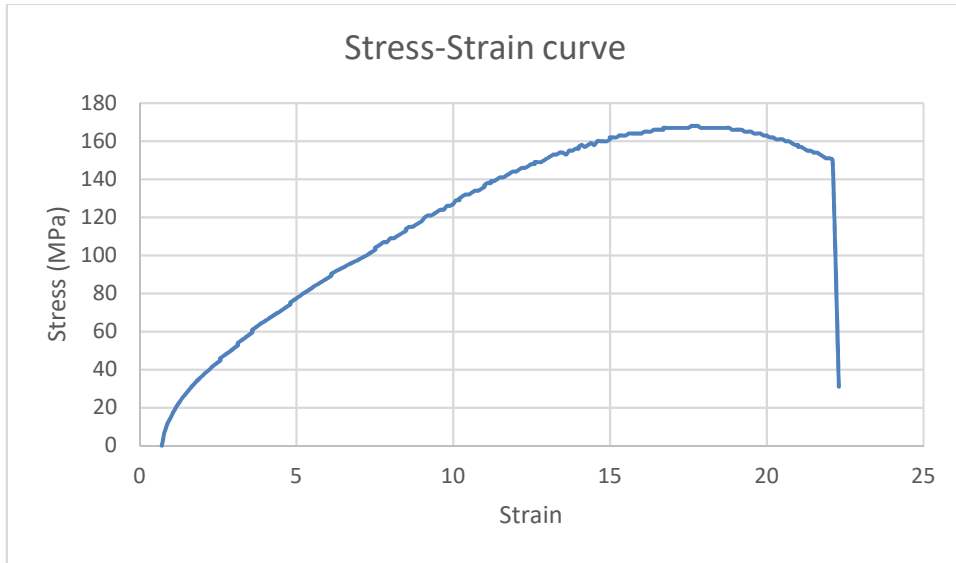
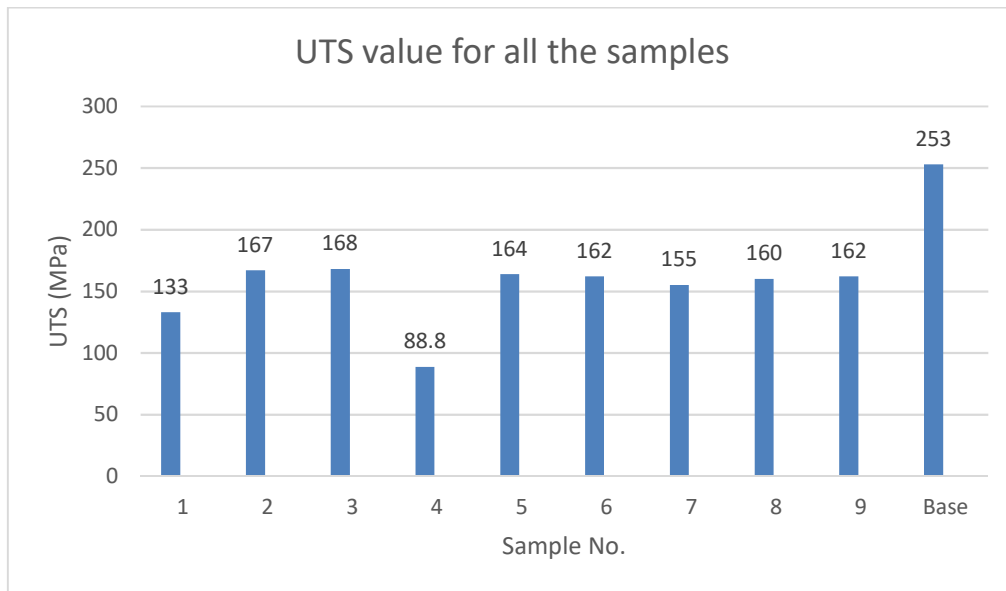Figure 4.8 Stress strain diagram for 3$^{rd}$ FSP over CMT welded sample



Figure 4.9 UTS value for all FSP over CMT welded samples

From both the tensile test analysis, it can be clearly seen that UTS for the CMT sample is higher from the UTS of the FSP over CMT samples [44] for higher value of WC (190 A). Samples which are CMT welded at 190 A WC have better strength compared to the same samples on which FSP was also done while samples which are welded at 170 A WC and FSP was done on them, they show better strength. But highest UTS of CMT sample is more than

the FSP over CMT sample. FSP samples are showing a range of 155 – 165 MPa and they are not going above that value despite of any change in process parameter.

## 4.3    Microhardness test

Microhardness test was conducted on the top 3 samples who have the highest UTS among all the samples for both the processes. This means sample number 7, 8, and 9 were chosen from all the samples which were processed by CMT process and sample number 1, 2, and 3 were chosen from all the samples which were processed by FSP over CMT process. Hardness values were calculated at BM (point 1 & 7), HAZ (point 2 & 6), & WZ (point 3, 4, & 5) for CMT welding process and at SZ (point 3 & 4), TMAZ (point 2 & 5), and BM (point 1 & 2) for FSP over CMT samples as shown in Fig. 4.10 and Fig. 4.11 respectively.
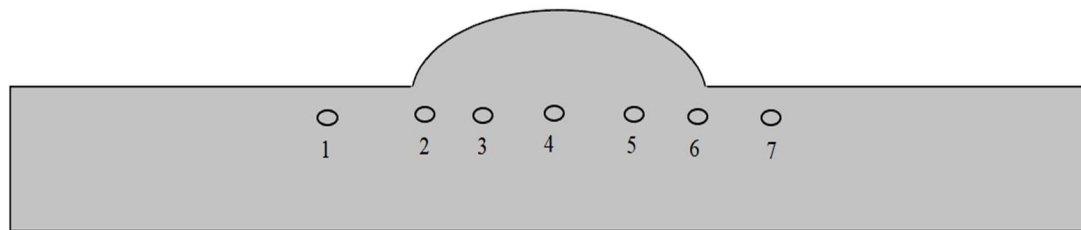


Figure 4.10 Hardness testing points for CMT sample



Figure 4.11 Hardness testing points for FSP over CMT samples

Hardness value was also checked for the BM as UTS was checked for the BM. The value of Microhardness for the BM is 69.88 HV which was average of three points on two samples.

### 4.3.1    Microhardness test of CMT samples

The three samples that have been selected for the Microhardness test were sample number 7, 8, and 9 as they have the highest UTS among all other samples. Process parameters used for these samples are shown in Table 4.9 below.

Table 4.9 Selected CMT samples for Microhardness test

| Sample No. | WC (A) | WS (cm/min) | GFR (L/min) | UTS (MPa) |
|---|---|---|---|---|
| 7 | 190 | 35 | 18 | 173 |
| 8 | 190 | 40 | 12 | 180 |
| 9 | 190 | 45 | 15 | 192 |

For Microhardness test, a load of 500 gram was applied on the sample for a dwelling period of 10 sec. 2 indentation were made on BM, 2 indentation were made on HAZ, and 3 indentation were made on WZ. Hence, total 7 indentation were made on all over the sample. The hardness value at different points and regions are shown in Table 4.10 and comparative hardness value for all three samples at different zones are shown in fig. 4.12 and hardness value for 9th sample at different points is shown in Fig. 4.13.

Table 4.10 Hardness value of top three CMT samples

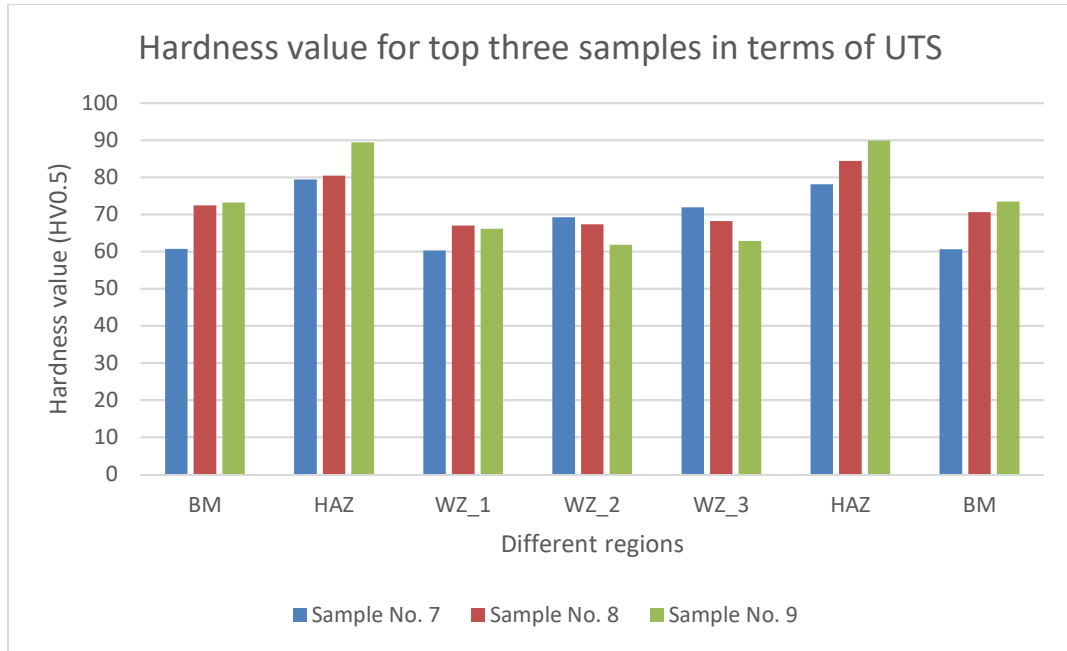| Point No. | Region | Hardness value for sample no 7 (HV0.5) | Hardness value for sample no 8 (HV0.5) | Hardness value for sample no 9 (HV0.5) |
|---|---|---|---|---|
| 1 | BM | 60.66 | 72.37 | 73.17 |
| 2 | HAZ | 79.43 | 80.42 | 89.41 |
| 3 | WZ_1 | 60.27 | 66.96 | 66.08 |
| 4 | WZ_2 | 69.19 | 67.36 | 61.85 |
| 5 | WZ_3 | 71.86 | 68.18 | 62.82 |
| 6 | HAZ | 78.06 | 84.43 | 89.81 |
| 7 | BM | 60.61 | 70.59 | 73.47 |

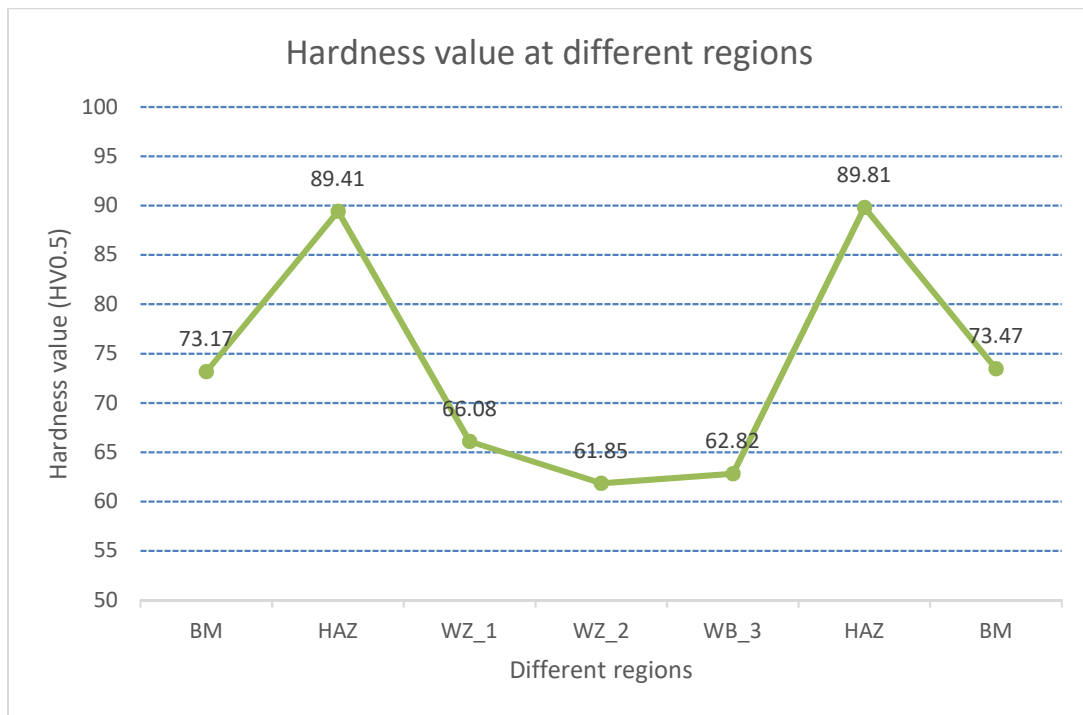Figure 4.12 Comparative Hardness value for sample 7, 8, & 9



Figure 4.13 Hardness value for 9$^{th}$ sample at different region

The microhardness value of the WZ was found out to be less than the BM because of grain size refinement. Maximum value of hardness is coming to be 89.61 HV (average of two) at

HAZ while it was 63.58 HV (average of three on WZ) for WZ for the 9th sample. Hardness value of WZ is lower than the HAZ & BM because of the rapid cooling rate, grains became finer. The rapid cooling rate is because the heat input decreases as we move from WZ to HAZ, which leads to growth of reduced grain size [40]. Diamond indenter indentation marks for the 9th sample are shown in Fig. 4.14.
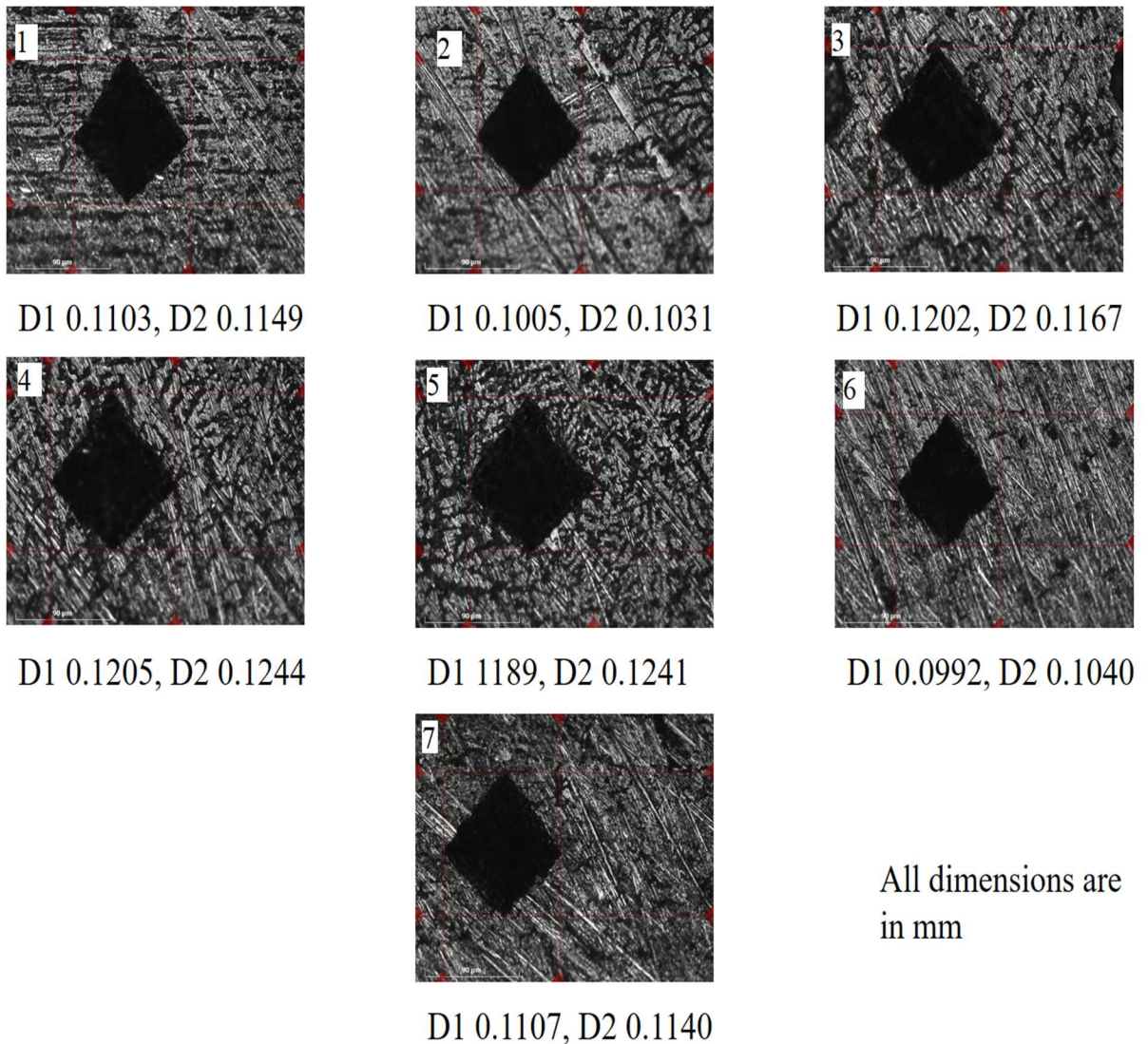


D1 0.1103, D2 0.1149          D1 0.1005, D2 0.1031          D1 0.1202, D2 0.1167

D1 0.1205, D2 0.1244          D1 1189, D2 0.1241          D1 0.0992, D2 0.1040

All dimensions are in mm

D1 0.1107, D2 0.1140

Figure 4.14 Indentation marks on sample number 9

From the Microhardness test conducted on the CMT welded sample, it can be seen that the hardness value first increases sharply at HAZ, then decreases sharply for the WZ, then again increases sharply at HAZ, and finally decreases sharply at the BM, Thus, making a M-pattern.

### 4.3.2 Microhardness test of FSP over CMT samples

The three samples that have been selected for the Microhardness test were sample number 2, 3, and 5 as they have the highest UTS among all other samples. Process parameters used for these samples are shown in Table 4.11 below.

Table 4.11 FSP over CMT samples for Microhardness test

| S. No. | WC (A) | WS (cm/min) | GFR (L/min) | TTS (mm/min) | TRS (rpm) | UTS (MPa) |
|--------|--------|-------------|-------------|--------------|-----------|-----------|
| 2 | 170 | 40 | 15 | 80 | 1000 | 167 |
| 3 | 170 | 45 | 18 | 80 | 700 | 168 |
| 5 | 180 | 40 | 18 | 60 | 1000 | 164 |

For Microhardness test, similar to CMT sample, a load of 500 gram was applied on the sample for a dwelling period of 10 sec. 2 indentation were made on BM, 2 indentation were made on TMAZ, and 2 indentation were made on SZ. Hence, total 6 indentation were made on all over the sample. The hardness value at different points and regions are shown in Table 4.12 and comparative hardness value for all three samples at different zones are shown in fig. 4.15 hardness value at different regions is shown in Fig. 4.16.

Table 4.12 Hardness value of top three FSP over CMT samples

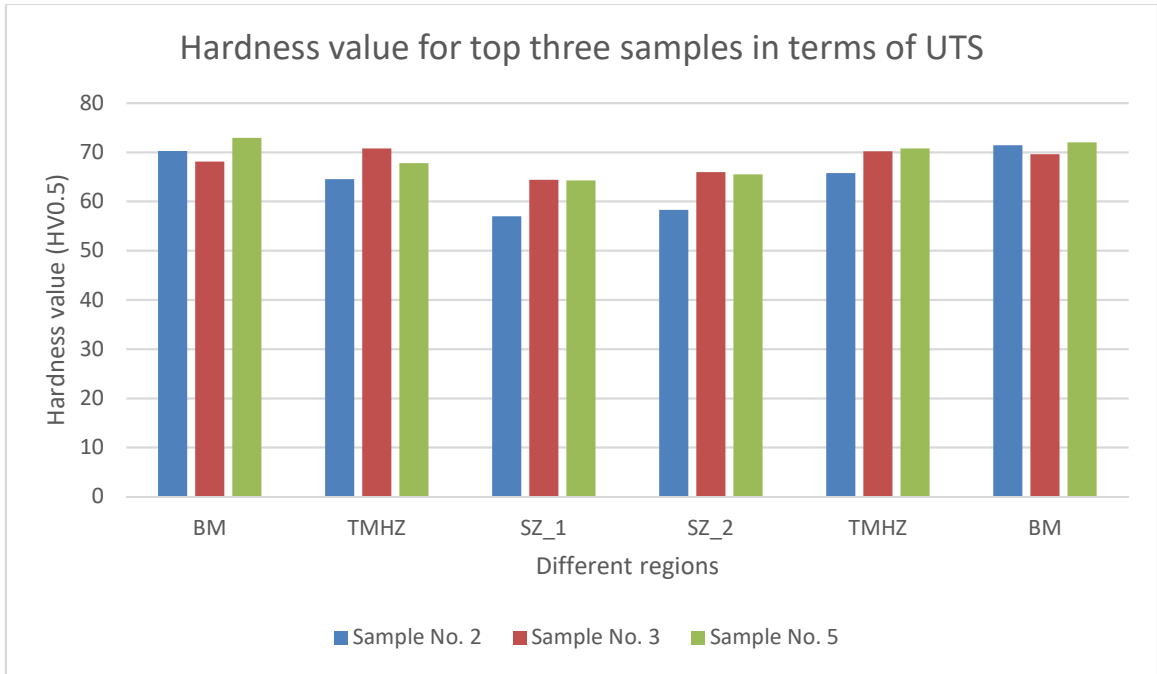| Point no. | Region | Hardness value for sample no. 2 (HV0.5) | Hardness value for sample no. 3 (HV0.5) | Hardness value for sample no. 5 (HV0.5) |
|-----------|--------|-----------------------------------------|-----------------------------------------|-----------------------------------------|
| 1 | BM | 70.25 | 68.09 | 72.93 |
| 2 | TMHZ | 64.51 | 70.73 | 67.74 |
| 3 | SZ_1 | 56.97 | 64.39 | 64.29 |
| 4 | SZ_2 | 58.28 | 65.96 | 65.49 |
| 5 | TMHZ | 65.73 | 70.17 | 70.79 |
| 6 | BM | 71.4 | 69.57 | 72.02 |

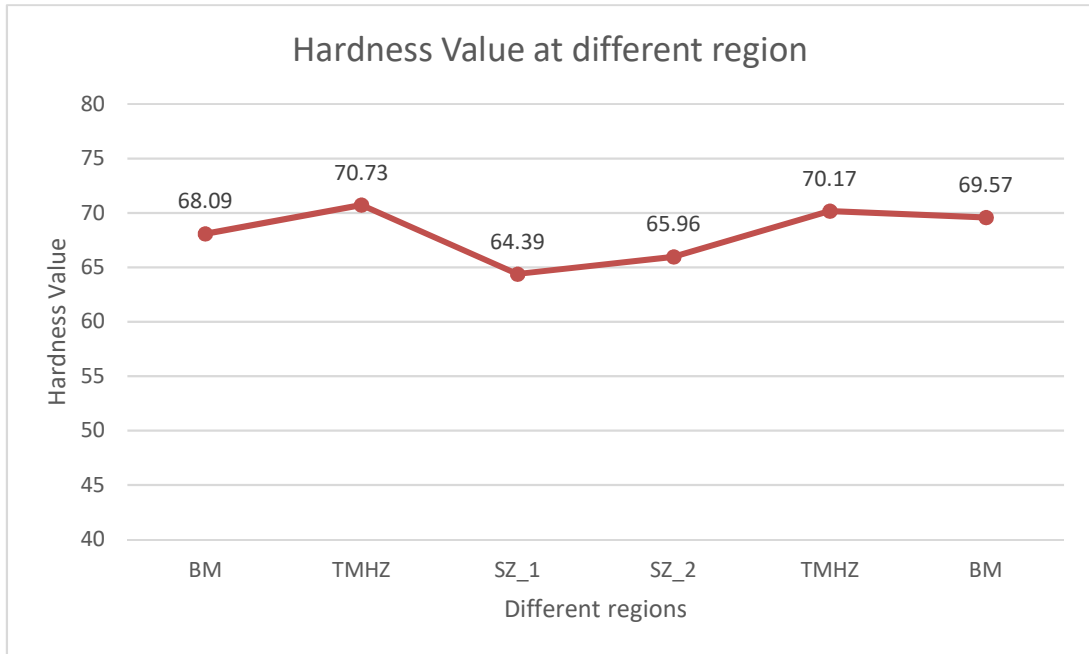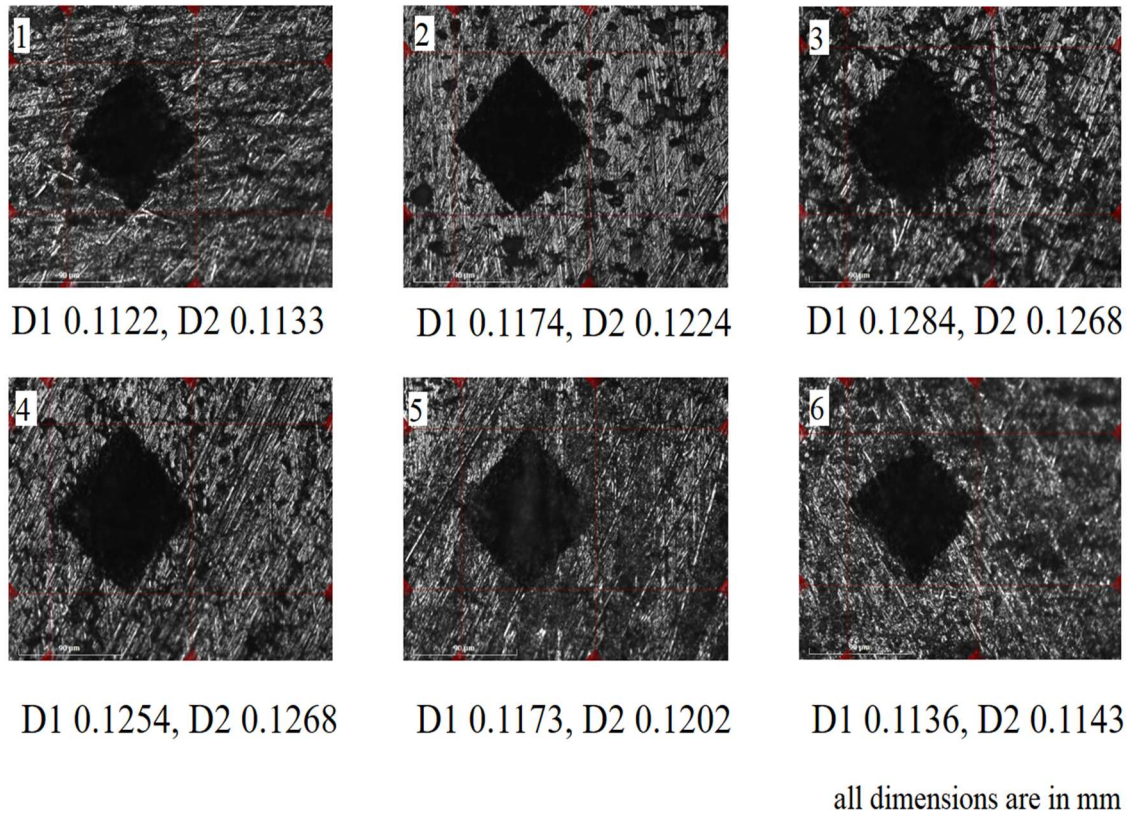Figure 4.15 Comparative Hardness value for sample 2, 3, & 5



Figure 4.16 Hardness value for 3$^{rd}$ sample at different region

The microhardness value of SZ was found out to be less than compared to this sample BM. Maximum value of hardness is coming to be 70.45 HV (average of two) at TMAZ while it was 65.18 HV (average of two) on SZ for the 3$^{rd}$ sample. Reduction of 5% in the hardness

value of SZ can be seen compared with the base metal. Diamond indenter indentation marks for the 3$^{rd}$ sample are shown in Fig. 4.17.



D1 0.1122, D2 0.1133      D1 0.1174, D2 0.1224      D1 0.1284, D2 0.1268

D1 0.1254, D2 0.1268      D1 0.1173, D2 0.1202      D1 0.1136, D2 0.1143

all dimensions are in mm

Figure 4.17 Indentation marks on sample number 3

From the Microhardness test conducted on the CMT welded sample, it can be seen for 3$^{rd}$ sample that the hardness value first increases at TMAZ, then decreases for the SZ, then again increases at TMAZ, and finally decreases at the BM, Thus, making a M-pattern. For both the processes weld zone i.e., WZ for CMT sample and SZ for FSP over CMT sample, hardness value was found less than the BM hardness value [41]. It can also be noted that the value of hardness increases with increase in TRS [46]. It can be seen that the hardness value of the WZ for CMT samples was 63.58 HV while harness value at SZ for FSP over CMT samples was 65.18 HV. Though the increment in hardness value is small (2.5%) but it increases. Hence, FSP over CMT samples can be helpful in increasing its hardness value.

## 4.4    Microstructure analysis

Microstructure analysis was done only for those samples which have the highest value of UTS, as it was done for Microhardness test. Majorly three regions where there which were focused for the study and analysis of microstructure for both the processes. For CMT sample, it was BM, HAZ, and WZ while for FSP over CMT samples, it was BM, TMAZ, and SZ. Olympus microscope has been used for the study with 100X, 200X, and 500X scale lens.

### 4.4.1    Microstructure analysis of CMT samples

Most optimized sample was selected, who have the maximum tensile stress (sample no $9^{th}$), for the microstructure analysis. Below are the images of the microstructure on different zoom level.
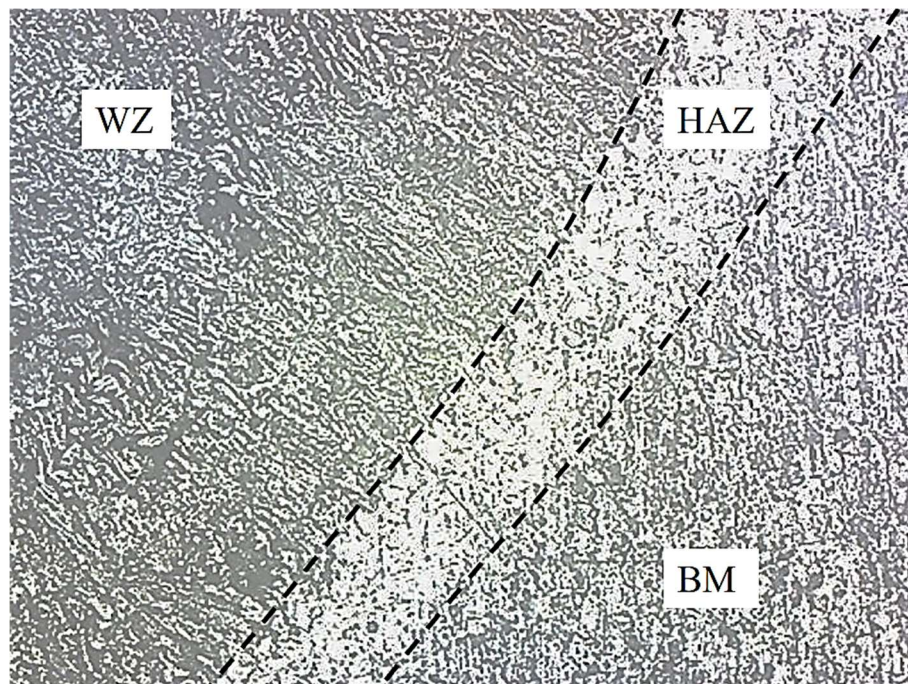


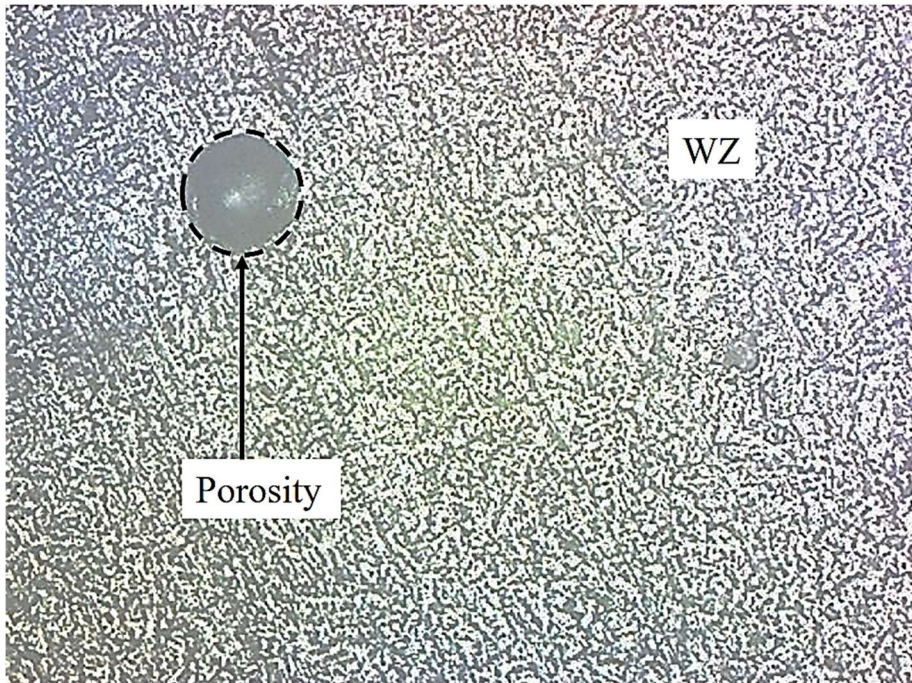Figure 4.18 WZ, HAZ, & BM at 100X zoom
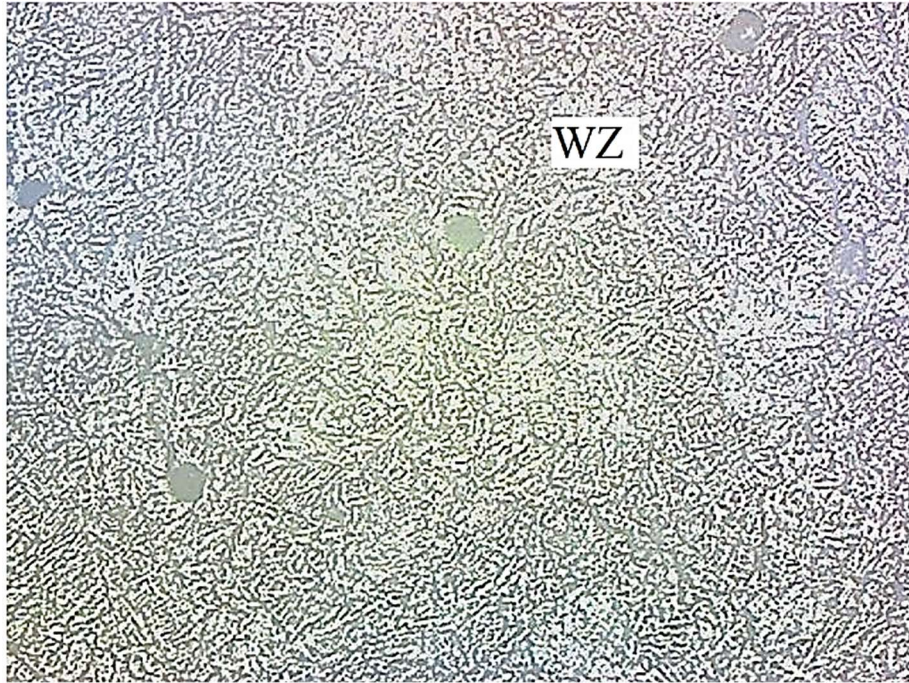
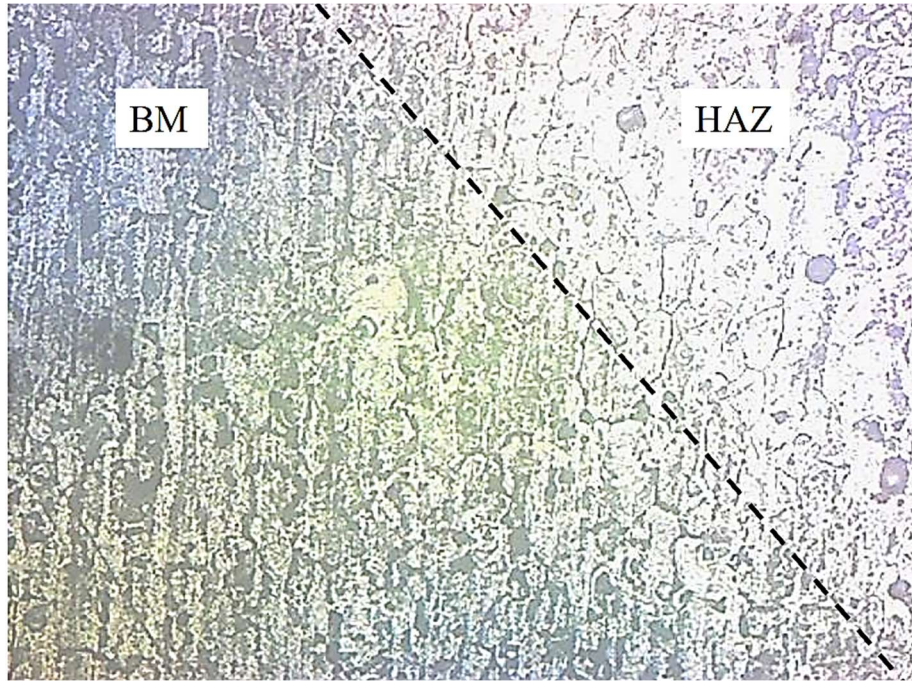Figure 4.19 WZ at 100X zoom



Figure 4.20 WZ at 100X zoom

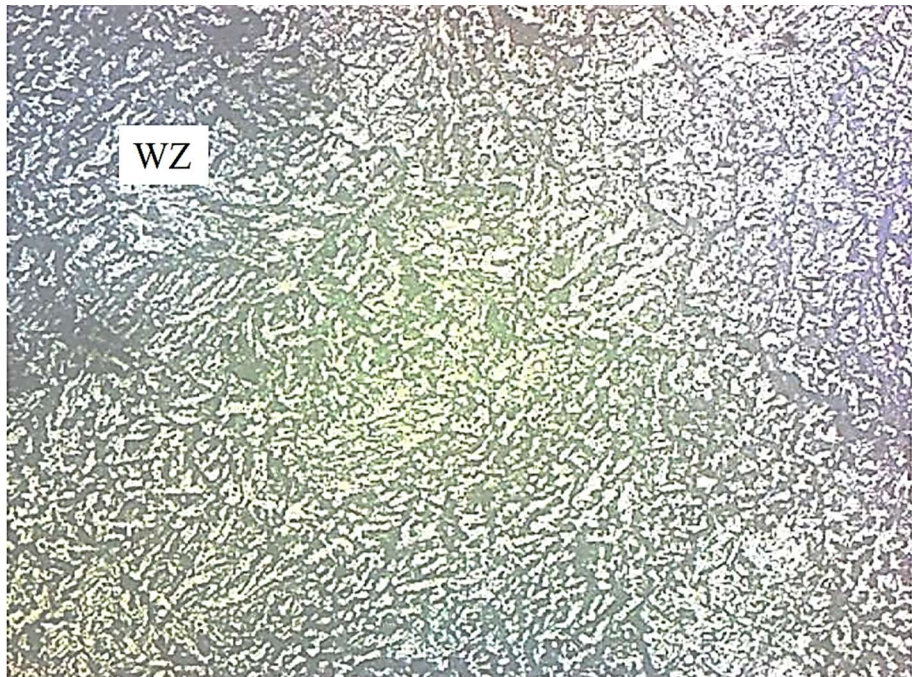Figure 4.21 BM & HAZ at 200X zoom



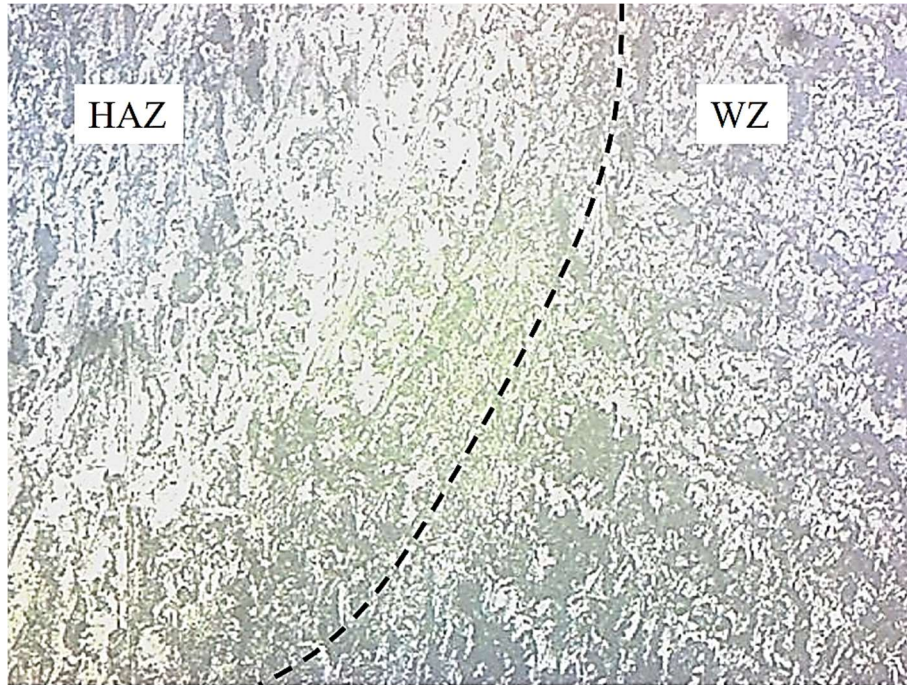Figure 4.22 WZ at 200X zoom
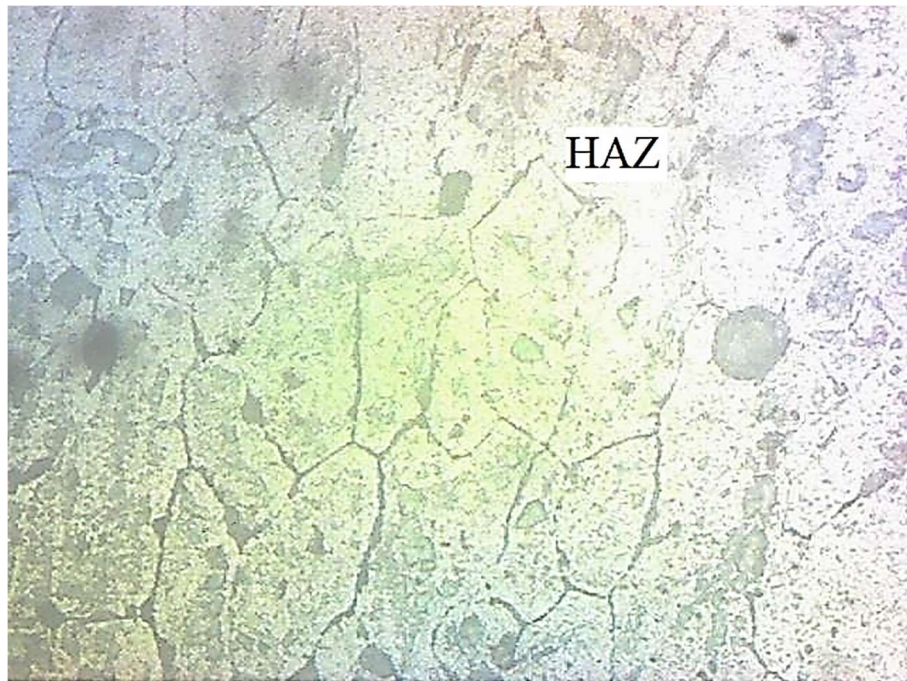
Figure 4.23 HAZ & WZ at 200X zoom
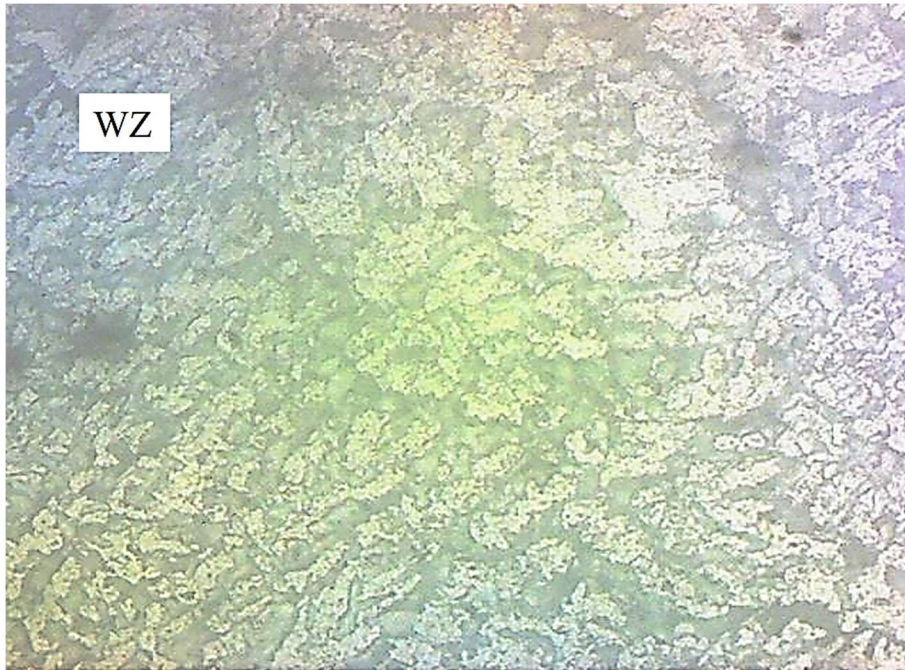


Figure 4.24 HAZ at 500X zoom
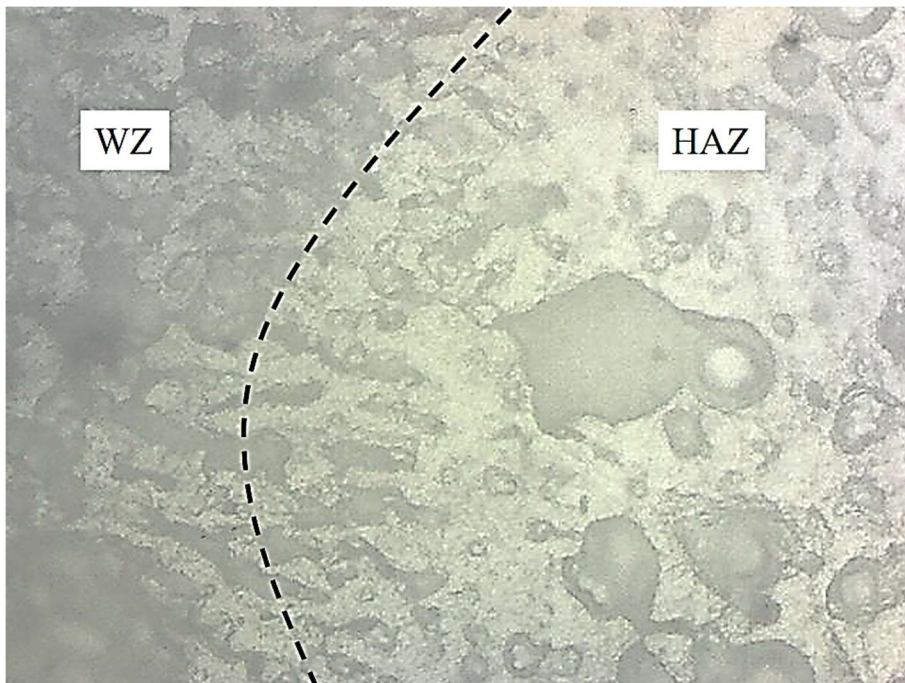
Figure 4.25 WZ at 500X zoom



Figure 4.26 WZ & HAZ at 500X zoom

Above images shown were microstructure images at 100X, 200X, & 500X zoom for CMT welded sample using AA6082 material and ER5356 filler wire in butt configuration. The

dark patches that are showing in Fig. 4.24 & 4.25 are dark dendrites with fine particles of Mg3Al2 and this is a common phenomenon while using ER5356 as a filler wire [11]. While in fig. 4.20 porosity with equiaxed grain structure can be seen. During CMT welding, there is partial melting of grain boundaries occurred due to which fusion occur within the joint [42]. As the heat input decreases from WZ to HAZ, cooling rate increases and hence, grain refinement occurred and hence columnar grain structure is present in HAZ and equiaxed grain structure is present in WZ. This microstructure analysis also suggests that porosity is present in weld bead which could be a reason for lower UTS compared to base metal.

### 4.4.2   Microstructure analysis of FSP over CMT samples

Most strong sample was selected, who have the maximum tensile stress (sample no $3^{rd}$), for the microstructure analysis. Below are the images of the microstructure on different zoom level.
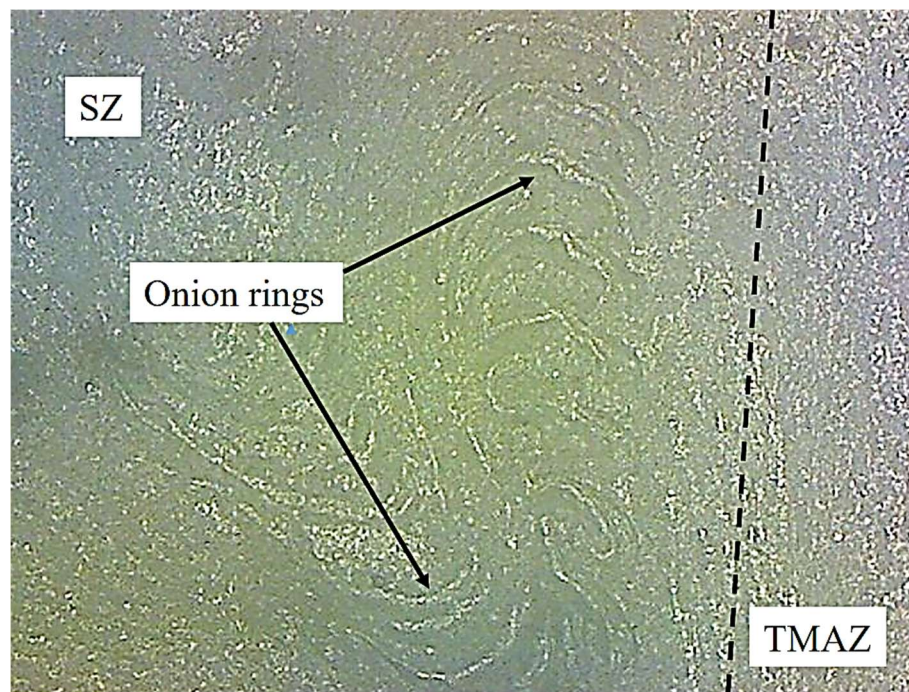


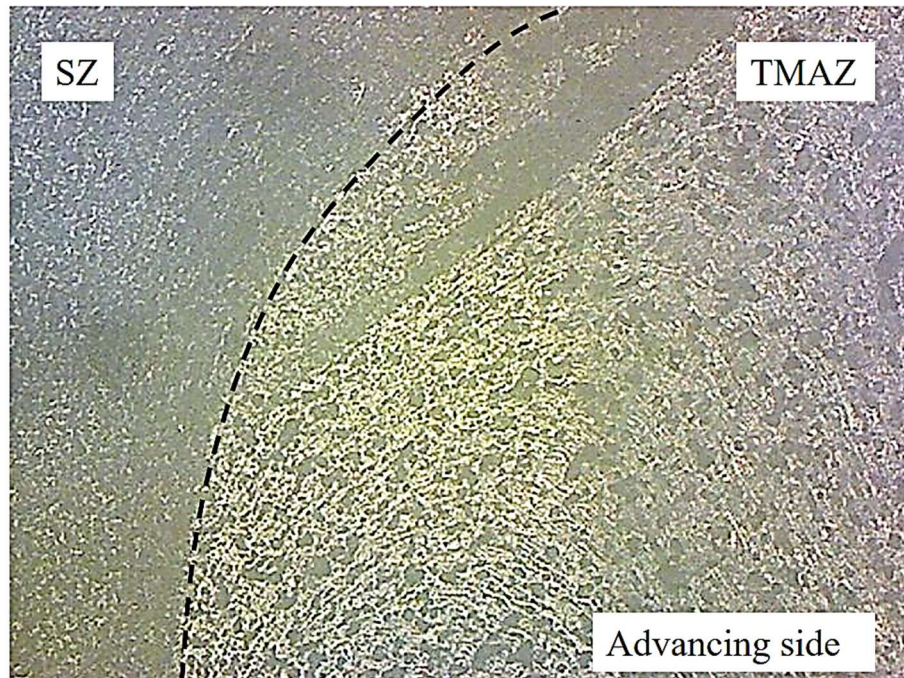Figure 4.27 SZ & TMAZ at 100X zoom

Figure 4.28 SZ & TMAZ at 100X zoom



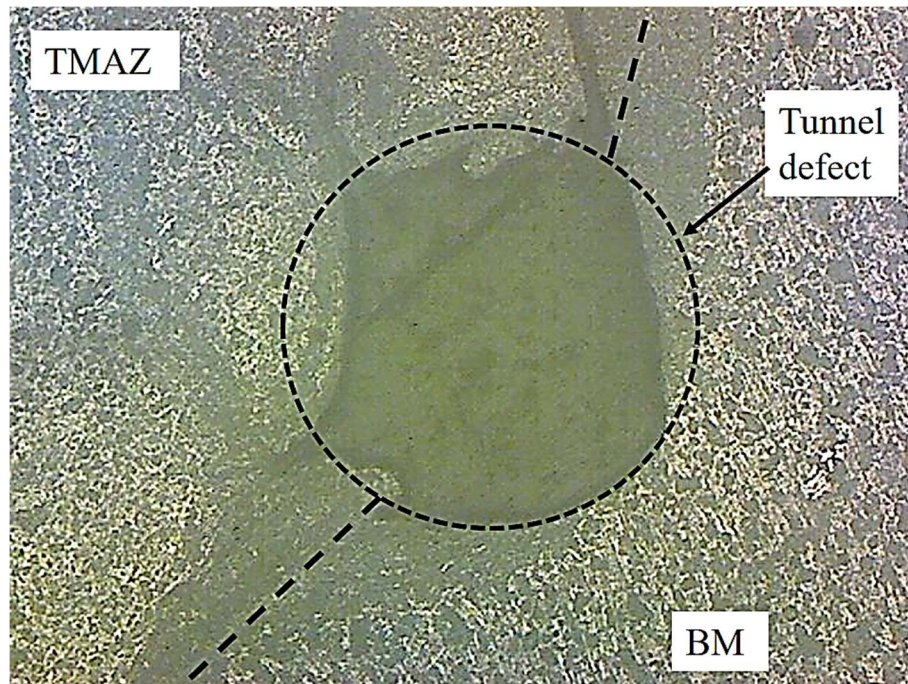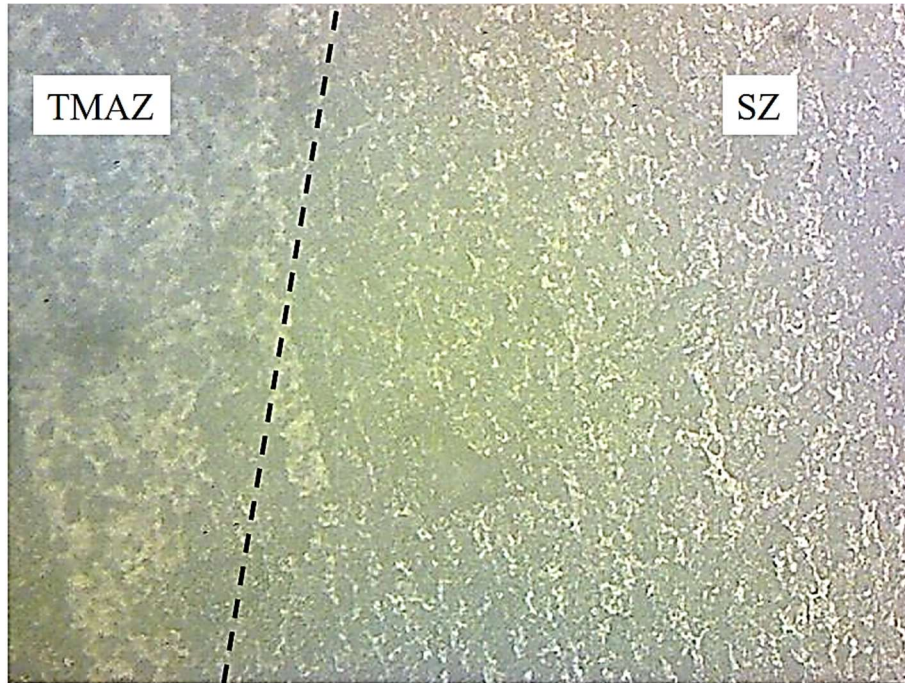Figure 4.29 BM & TMAZ at 100X zoom

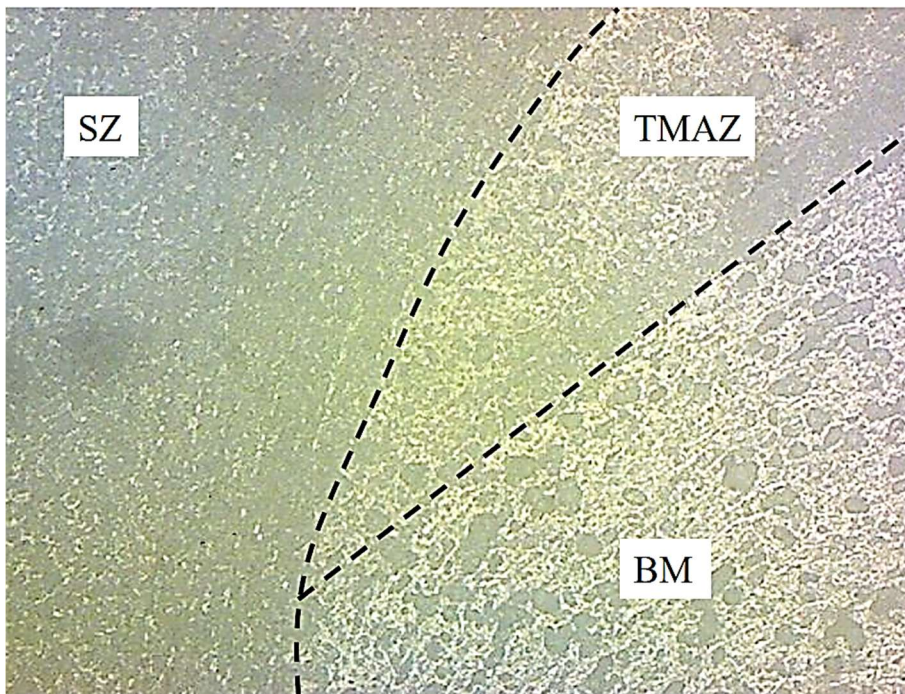Figure 4.30 TMAZ & SZ at 200X zoom



Figure 4.31 SZ, TMAZ, & BM at 200X zoom
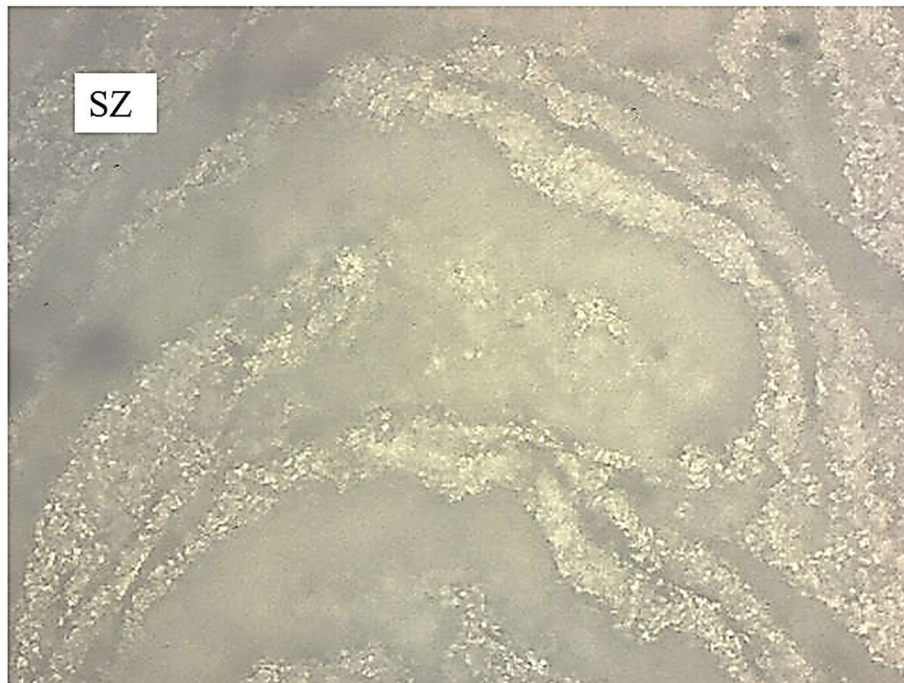
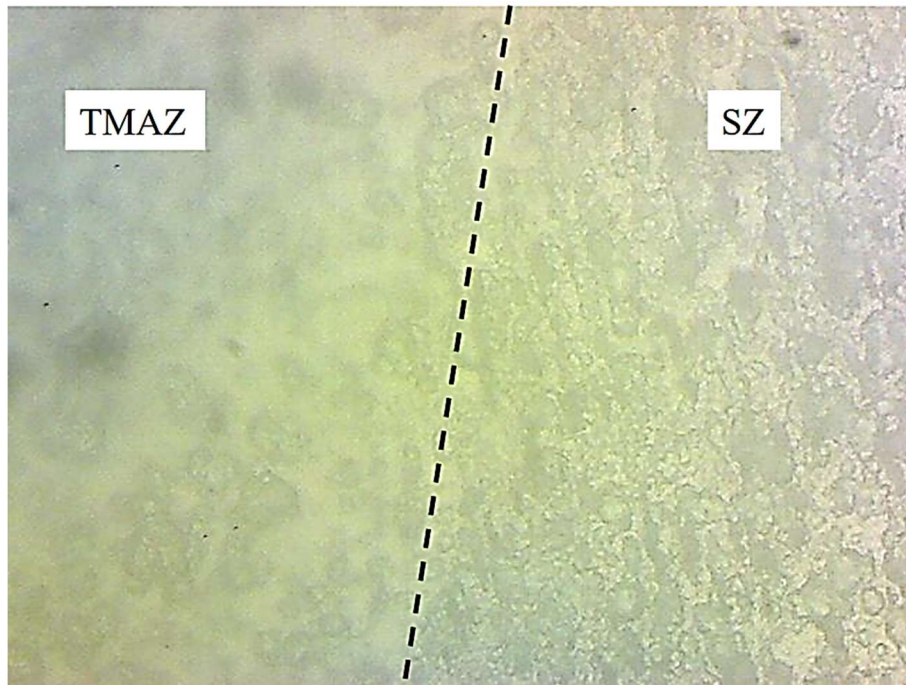Figure 4.32 SZ at 200X zoom



Figure 4.33 SZ at 500X zoom

Figure 4.34 TMAZ & SZ at 500X zoom
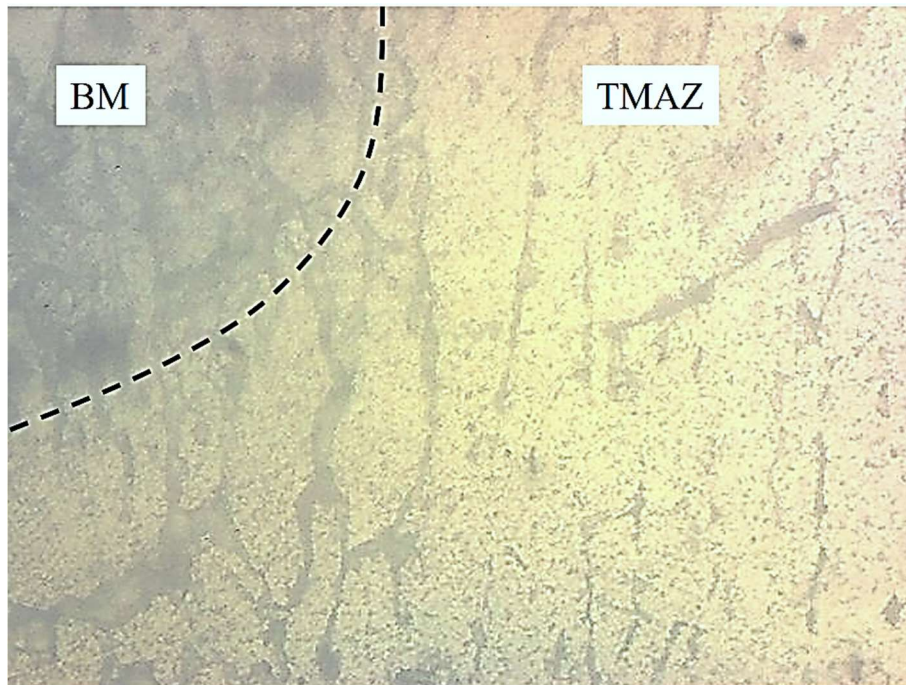


Figure 4.35 BM & TMAZ at 500X zoom

Above images shown were microstructure images at 100X, 200X, & 500X zoom for FSP over CMT welded sample using AA6082 material and ER5356 filler wire in butt

configuration. Grains at TMAZ are coarser while grains at SZ are very fine. This is because there is intense plastic deformation and temperature increases heating due to friction. Hence, formation of recrystallized fine grain structure occur in the SZ. The same phenomenon can be seen in [46] where grains became fine when FSP was done on GSTW. Material transportation occurs as the formation of onion rings in the SZ are there. At lower TTS and TRS, SZ was subjected to maximum temperature due to the additional stirring time which reduces the grain size [47]. While porosity was absent in the FSP over CMT samples, but at higher TRS, tunnel defects were observed which were the reason for the lower value of UTS were over the BM. TRS has much more influence on the tunnel void area compared to TTS [48]. At higher TRS, tunnel defects have been seen in experiment. These tunnel defects can be minimized by increasing the number of passes due to recrystallization mechanism but this indirectly decreases the UTS at SZ [49].

# CHAPTER 5

# CONCLUSION

In this research work, 5 mm thick plate of aluminium alloy AA6082-T6 has been butt welded using ER5356 as a filler wire material using two techniques and different process parameters. Total 18 samples were there (9 for CMT & 9 for FSP over CMT) which were welded using DoE table and process parameters were optimized using Taguchi optimization method. Mechanical tensile test, microhardness distribution, and microstructure analysis were done on the samples and from that following conclusion were observed:

1. Sample of 5 mm thick AA6082 aluminium plate were successfully welded using CMT welding and FSP was successfully done on them upto half of sample length. Taguchi method was used to optimize the process parameters for both the processes.
2. The optimized process parameter for the CMT welded joint comes out at 190 A WC, 40 cm/min WS, & 15 L/min GFR. On this optimized value of process parameters, Taguchi predicted UTS value was coming to be 205.64 MPa which was 81.28% of BM. Also, ANOVA results show that WC have more effect on UTS with a contribution of 67.47%.
3. The optimized process parameter for the FSP over CMT welded joint comes out at 40 mm/min TTS & 700 rpm TRS. . On this optimized value of process parameters, Taguchi predicted UTS value was coming to be 171.911 MPa which was 67.49% of BM. Also, ANOVA results show that TRS have more effect on UTS with a contribution of 50.45%.
4. In case of CMT welding, hardness value of HAZ was highest followed by BM and WZ. Hardness value of WZ was lowest due to rapid cooling, grains became finer. In case of FSP over CMT welding, as TRS increases, the value of hardness was also find to be increased. Performing FSP over CMT welded samples increase the microhardness level by small percentage (2.51%) as it refine the grain structure by dynamic recrystallization. The microhardness distribution was making an M-pattern for both the processes.

5. By doing the microstructure analysis of CMT sample, we find equiaxed grain structure with dendrites of fine Mg3Al2 particles in the WZ while columnar grain structure was present in the HAZ. The dark dendrites are commonly present when welding is done using ER5356 filler wire while the difference the grain structure between WZ and HAZ is due to cooling rate and heat input. Gas porosities were found in the WZ which can decrease the UTS value.

6. FSP over CMT sample microstructure shows gains at TMAZ were coarser while grains at SZ were extremely fine due to the stirring effect that causes heavy plastic deformation and dynamic recrystallization occurs in SZ. Onion rings formation gives proof to the fact that material transportation is occurring. FSP has removed defects like gas porosities and lack of fusion thus, refining the microstructure. But at higher TRS, tunnel defects were found which limiting the UTS of the FSP over CMT welded samples.

## 5.1. Future scope

There is extensive scope of this research that can be explored since there are two process used to weld the 5 mm thick AA6082 aluminium alloy using ER5356 filler wire. They are as follow:

1. During welding, generally residual stresses and distortion generates. It can be further tested for the same and studied deeply to reduce it.

2. To maintain a good quality weld, effect pre-heating and post-heating the welded specimen can also be investigated. This can remove gas porosity and can give more improved UTS results.

3. Same experiment can also be performed by taking a V-slot on aluminium alloy plates. This will be helpful in removing the lack of fusion condition and can give better UTS results.

4. SEM, EDS, Fratography test can also be conducted to understand the microstructure and nature of breaking of sample.

# REFERENCES

[1] Mehul Pathak, & A.K. Madan. (2021). Role of Additive Manufacturing, Augmented Reality, Internet of Things in building Industry 4.0. International Journal of Research in Aeronautical and Mechanical Engineering, 9(10), 23–44. https://doi.org/10.5281/zenodo.5651851

[2] Omid Ferdowsi Hosseinabadi, Mohammad Reza Khedmati, A review on ultimate strength of aluminium structural elements and systems for marine applications, Ocean Engineering, Volume 232, 2021, 109153, ISSN 0029-8018, https://doi.org/10.1016/j.oceaneng.2021.109153.

[3] Rajesh P. Verma, Manish Kumar Lila, A short review on aluminium alloys and welding in structural applications, Materials Today: Proceedings, Volume 46, Part 20, 2021, Pages 10687-10691, ISSN 2214-7853, https://doi.org/10.1016/j.matpr.2021.01.447.

[4] Marek Stanisław Węglowski, Friction stir processing – State of the art, Archives of Civil and Mechanical Engineering, Volume 18, Issue 1, 2018, Pages 114-129, ISSN 1644-9665, https://doi.org/10.1016/j.acme.2017.06.002.

[5] G. Mathers, The welding of aluminium and its alloys, Woodhead Publishing Limited, 2002

[6] Rajesh P. Verma, K.N. Pandey, Kovács András, Rohit Khargotra, Tej Singh, Difficulties and redressal in joining of aluminium alloys by GMA and GTA welding: a review, Journal of Materials Research and Technology, Volume 23, 2023, Pages 2576-2586, ISSN 2238-7854, https://doi.org/10.1016/j.jmrt.2023.01.183.

[7] R. Cao, Gang Yu, J.H. Chen, Pei-Chung Wang, Cold metal transfer joining aluminum alloys-to-galvanized mild steel, Journal of Materials Processing Technology, Volume 213, Issue 10, 2013, Pages 1753-1763, ISSN 0924-0136, https://doi.org/10.1016/j.jmatprotec.2013.04.004.

[8] S. Babu, S.K. Panigrahi, G.D. Janaki Ram, P.V. Venkitakrishnan, R. Suresh Kumar, Cold metal transfer welding of aluminium alloy AA 2219 to austenitic stainless steel AISI 321, Journal of Materials Processing Technology, Volume 266, 2019, Pages 155-164, ISSN 0924-0136, https://doi.org/10.1016/j.jmatprotec.2018.10.034.

[9] Sravanthi S.S., Swati Ghosh Acharyya, Phani Prabhakar K.V., Padmanabham G., Integrity of 5052 Al-mild steel dissimilar welds fabricated using MIG-brazing and cold metal transfer in nitric acid medium, Journal of Materials Processing Technology, Volume 268, 2019, Pages 97-106, ISSN 0924-0136, https://doi.org/10.1016/j.jmatprotec.2019.01.010.

[10] Shanglu Yang, Jing Zhang, Jin Lian, Yongpin Lei, Welding of aluminum alloy to zinc coated steel by cold metal transfer, Materials & Design, Volume 49, 2013, Pages 602-612, ISSN 0261-3069, https://doi.org/10.1016/j.matdes.2013.01.045.

[11] Beytullah Gungor, Erdinc Kaluc, Emel Taban, Aydin SIK ŞŞ, Mechanical and microstructural properties of robotic Cold Metal Transfer (CMT) welded 5083-H111 and 6082-T651 aluminum alloys, Materials & Design (1980-2015), Volume 54, 2014, Pages 207-211, ISSN 0261-3069, https://doi.org/10.1016/j.matdes.2013.08.018.

[12] S. Sivabalan, R. Sridhar, G. Sathishkumar, Study on mechanical behaviour of friction stir welded 6082-T6 aluminium alloys, Materials Today: Proceedings, Volume 69, Part 3 2022, Pages 944-949, ISSN 2214-7853, https://doi.org/10.1016/j.matpr.2022.07.379.

[13] PavanKumar Thimmaraju, Krishnaiah Arkanti, G.ChandraMohan Reddy, K.B.G.Tilak, Comparison of Microstructure and Mechanical Properties of friction Stir welding of Al 6082 aluminum alloy with different Tool Profiles, Materials Today: Proceedings, Volume 3, Issue 10, Part B, 2016, Pages 4173-4181, ISSN 2214-7853, https://doi.org/10.1016/j.matpr.2016.11.092.

[14] Sipokazi Mabuwa, Velaphi Msomi, "Effect of Friction Stir Processing on Gas Tungsten Arc-Welding and Friction Stir-Welded 5083-H111 Aluminium Alloy Joints", Advances in Materials Science and Engineering, vol. 2019, Article ID 3510236, 14 pages, 2019. https://doi.org/10.1155/2019/3510236.

[15] Nafeez Ahmed Liyakat, Dhinakaran Veeman, Improvement of mechanical and microstructural properties of AA 5052-H32 TIG weldment using friction stir processing

approach, Journal of Materials Research and Technology, Volume 19, 2022, Pages 332-344, ISSN 2238-7854, https://doi.org/10.1016/j.jmrt.2022.05.015.

[16] Gao, K., Liu, G., H. et al. Experimental Investigation and Optimization on the Process Parameters during Induction Pressure Welding for Steel and Aluminium Alloy Using Response Surface Method. J. of Materi Eng and Perform 31, 6572-6583 (2022). https://doi.orgg/10.1007/s11665-022-06734-3

[17] K Furukawa (2006) New CMT arc welding process – welding of steel to aluminium dissimiliar metals and welding of super-thin aluminium sheets, Welding International, 20:6, 440-445, DOI: https://doi.ord/10.1533/wint.2006.3598

[18] S. Selvi, A. Vishvaksenan, E. Rajasekar, Cold metal transfer (CMT) technology - An overview, Defence Technology, Volume 14, Issue 1, 2018, Pages 28-44, ISSN 2214-9147, https://doi.org/10.1016/j.dt.2017.08.002.

[19] Jicai Feng, Hongtao Zhang, Peng He, The CMT short-circuiting metal transfer process and its use in thin aluminium sheets welding, Materials & Design, Volume 30, Issue 5, 2009, Pages 1850-1852, ISSN 0261-3069, https://doi.org/10.1016/j.matdes.2008.07.015.

[20] Rosado T, Almeida P, Pires I, Miranda R, Quintino L. Innovation in arc welding, Congresso de Engenharia de Moçambique, Maputo, Septembro 2–4; 2008. [REF: 44A004].

[21] Liang Zhang, Songtao Wang, Huixia Wang, Jun Wang, Tianshun Wang, Xuerui Dai, Investigate the effect of arc characteristic on the mechanical properties of 5A56 Al alloy in CMT arc additive manufacturing, CIRP Journal of Manufacturing Science and Technology, Volume 40, 2023, Pages 102-113, ISSN 1755-5817, https://doi.org/10.1016/j.cirpj.2022.10.006.

[22] Murr, L.E. A Review of FSW Research on Dissimiliar Metal and Alloy System. J. of Materi Eng and Perform 19, 1071-1089 (2010). https://doi.org/10.1007/s11665-010-9598-0.

[23] Harshadkumar H. Jadav, Vishvesh Badheka, Daulat Kumar Sharma, Gautam Upadhyay, A review on effect of friction stir processing on the welded joints, Materials Today: Proceedings, Volume 43, Part 1, 2021, Pages 84-92, ISSN 2214-7853, https://doi.org/10.1016/j.matpr.2020.11.215.

[24] Thomas, W.M., Johnson, K.I. and Wiesner, C.S. (2003), Friction Stir Welding – Recent Developments in Tool and Process Technologies. Adv. Eng. Mater., 5: 485-490. https://doi.org/10.1002/adem.200300355

[25] Liang Yin, Zhao-peng Ni, Ji-yang Liu, Feng Fan, Xu-dong Zhi, Ji-hong Ye, Yan-chong Pan, Yu-hang Guo, High-temperature mechanical properties of constructional 6082-T6 aluminum alloy extrusion, Structures, Volume 48, 2023, Pages 1244-1258, ISSN 2352-0124, https://doi.org/10.1016/j.istruc.2023.01.043.

[26] E M Stanciu et al 2017 IOP Conf. Ser.: Mater. Sci. Eng. **209** 01205, https://doi.org/10.1088/1757-899X/209/1/012051

[27] Xizhang Chen, Su, C., Wang, Y. et al. Cold Metal Transfer (CMT) Based Wire and Arc Additive Manufacturing (WAAM) System. J. Surf Investig. 12, 1278-1284 (2018). https://doi.org/10.1134/S102745101901004X

[28] A Rajesh Kannan, N. Siva Shanmugam, S Naveenkumar, Effect of Arc Length Correction on Weld Bead Geometry and Mechanical Properties of AISI 316L Weldments by Cold Metal Transfer (CMT) Process, Materials Today: Proceedings, Volume 18, Part 7, 2019, Pages 3916-3921, ISSN 2214-7853, https://doi.org/10.1016/j.matpr.2019.07.331.

[29] A. Rajesh Kannan, N. Siva Shanmugam, Yasam Palguna, B. Girinath, Wonjoo Lee, Jonghun Yoon, Effect of double-side welding on the microstructural characteristics and mechanical performance of dissimilar AA6061-AA5052 aluminium alloys, Materials Letters, Volume 331, 2023, 133444, ISSN 0167-577X, https://doi.org/10.1016/j.matlet.2022.133444.

[30] A. Gomez Ortega, L. Corona Galvan, F. Deschaux-Beaume, B. Mezrag & S. Rouquette (2018) Effect of process parameters on the quality of aluminium alloy Al5Si deposits in wire and arc additive manufacturing using a cold metal transfer process, Science and Technology of Welding and Joining, 23:4, 316-332, https://doi.org/10.1080/13621718.2017.1388995

[31] Fereidoon Marefat, Angshuman Kapil, Seyed Aref Banaee, Patrick Van Rymenant, Abhay Sharma, Evaluating shielding gas-filler wire interaction in bi-metallic wire arc additive manufacturing (WAAM) of creep resistant steel-stainless steel for improved

process stability and build quality, Journal of Manufacturing Processes, Volume 88, 2023, Pages 110-124, ISSN 1526-6125, https://doi.org/10.1016/j.jmapro.2023.01.046.

[32] Y.B. Liu, Q.J. Sun, H.B. Sang & J.C. Feng (2015) Microstructure and mechanical properties of cold metal transfer welded aluminium/nickel lap joints, Science and Technology of Welding and Joining, 20:4, 307-312, https://doi.org/10.1179/1362171815Y.0000000011

[33] Alfredo Suárez, Asier Panfilo, Eider Aldalur, Fernando Veiga, Pablo Gomez, Microstructure and mechanical properties of mild steel-stainless steel bimetallic structures built using Wire Arc Additive Manufacturing, CIRP Journal of Manufacturing Science and Technology, Volume 38, 2022, Pages 769-773, ISSN 1755-5817, https://doi.org/10.1016/j.cirpj.2022.06.018.

[34] Fang, Xuewei, Lijuan Zhang, Hui Li, Chaolong Li, Ke Huang, and Bingheng Lu., Microstructure Evolution and Mechanical Behavior of 2219 Aluminum Alloys Additively Fabricated by the Cold Metal Transfer Process, Materials, 2018, no. 11(5): 812. https://doi.org/10.3390/ma11050812

[35] Peng He, Xingwang Bai, Haiou Zhang, Microstructure refinement and mechanical properties enhancement of wire and arc additively manufactured 6061 aluminum alloy using friction stir processing post-treatment, Materials Letters, Volume 330, 2023, 133365, ISSN 0167-577X, https://doi.org/10.1016/j.matlet.2022.133365.

[36] Lee, Seung Hwan., Optimization of Cold Metal Transfer-Based Wire Arc Additive Manufacturing Processes Using Gaussian Process Regression, Metals, 2020, 10(4): 461. https://doi.org/10.3390/met10040461

[37] Guo-yin ZU, Ri-huan LU, Xiao-bing LI, Zhao-yang ZHONG, Xing-jiang MA, Ming-bo HAN, Guang-chun YAO, Three-point bending behavior of aluminum foam sandwich with steel panel, Transactions of Nonferrous Metals Society of China, Volume 23, Issue 9, 2013, Pages 2491-2495, ISSN 1003-6326, https://doi.org/10.1016/S1003-6326(13)62759-4.

[38] Chen Zhang, Yufei Li, Ming Gao, Xiaoyan Zeng, Wire arc additive manufacturing of Al-6Mg alloy using variable polarity cold metal transfer arc as power source, Materials Science and Engineering: A, Volume 711, 2018, Pages 415-423, ISSN 0921-5093, https://doi.org/10.1016/j.msea.2017.11.084.

[39] N. T. Kumbhar, K. Bhanumurthy, Friction Stir Welding of Al 5052 with Al 6061 Alloys, Journal of Metallurgy, vol. 2012, Article ID 303756, 7 pages, 2012. https://doi.org/10.1155/2012/303756.

[40] Koli, Y., Yuvraj, N., Aravindan, S. et al. CMT Joining of AA6061-T6 and AA6082-T6 andExamining Mechanical Properties and Microstructure Characterization. Trans Indian Inst Met 74, 313-329 (2021). https://doi.org/10.1007/s12666-020-02134-0.

[41] Vijaya Krishna Varma K., Baig Ismail, Ravi Kumar B.V.R., Venkata Ramana M., Effect of friction stir welding parameters on tool geometry and metallurgical properties of AA 6082-T6 weldments at different weld zones, Materials Today: Proceedings, Volume 45, Part 2, 2021, Pages 3195-3200, ISSN 2214-7853, https://doi.org/10.1016/j.matpr.2020.12.370.

[42] Gurmeet Singh, Amardeep S. Kang, Kulwant Singh, Jagtar Singh, Experimental comparison of friction stir welding process and TIG welding process for 6082-T6 Aluminium alloy, Materials Today: Proceedings, Volume 4, Issue 2, Part A, 2017, Pages 3590-3600, ISSN 2214-7853, https://doi.org/10.1016/j.matpr.2017.02.251.

[43] Rajendran, C., Srinivasan, K., Balasubramanian, V., Balaji, H. and Selvaraj, P., Evaluation of load-carrying capabilities of friction stir welded, TIG welded and riveted joints of AA2014-T6 aluminium alloy, Aircraft Engineering and Aerospace Technology, Vol. 91 No. 9, 2019, pp. 1238-1244. https://doi.org/10.1108/AEAT-11-2017-0233.

[44] Long Wan, Yongxian Huang, Weiqiang Guo, Shixiong Lv, Jicai Feng, Mechanical Properties and Microstructure of 6082-T6 Aluminum Alloy Joints by Self-support Friction Stir Welding, Journal of Materials Science & Technology, Volume 30, Issue 12, 2014, Pages 1243-1250, ISSN 1005-0302, https://doi.org/10.1016/j.jmst.2014.04.009.

[45] P.C. Arunakumara, H.N. Sagar, Bimal Gautam, Raji George, S. Rajeesh, A review study on fatigue behavior of aluminum 6061 T-6 and 6082 T-6 alloys welded by MIG and FS welding methods, Materials Today: Proceedings, Volume 74, Part 2, 2023, Pages 293-301, ISSN 2214-7853, https://doi.org/10.1016/j.matpr.2022.08.242.

[46] Long Wan, Yongxian Huang, Weiqiang Guo, Shixiong Lv, Jicai Feng, Mechanical Properties and Microstructure of 6082-T6 Aluminum Alloy Joints by Self-support

Friction Stir Welding, Journal of Materials Science & Technology, Volume 30, Issue 12, 2014, Pages 1243-1250, ISSN 1005-0302, https://doi.org/10.1016/j.jmst.2014.04.009.

[47] P. Sinha, S. Muthukumaran, S.K. Mukherjee, Analysis of first mode of metal transfer in friction stir welded plates by image processing technique, J. Mater. Process. Technol. 197 (2008) 17–21, https://doi.org/10.1016/j.jmatprotec.2007.06.013.

[48] J. Rasti, Study of the welding parameters effect on the tunnel void area during friction stir welding of 1060 aluminum alloy, Int. J. Adv. Manuf. Technol. 97 (2018) 2221–2230, https://doi.org/10.1007/s00170-018-1857-5.

[49] R. Senthilkumar, M. Prakash, N. Arun, A. Arul Jeyakumar, The effect of the number of passes in friction stir processing of aluminum alloy (AA6082) and its failure analysis, Applied Surface Science, Volume 491, 2019, Pages 420-431, ISSN 0169-4332, https://doi.org/10.1016/j.apsusc.2019.06.132.